



저작자표시-비영리-변경금지 2.0 대한민국

이용자는 아래의 조건을 따르는 경우에 한하여 자유롭게

- 이 저작물을 복제, 배포, 전송, 전시, 공연 및 방송할 수 있습니다.

다음과 같은 조건을 따라야 합니다:



저작자표시. 귀하는 원저작자를 표시하여야 합니다.



비영리. 귀하는 이 저작물을 영리 목적으로 이용할 수 없습니다.



변경금지. 귀하는 이 저작물을 개작, 변형 또는 가공할 수 없습니다.

- 귀하는, 이 저작물의 재이용이나 배포의 경우, 이 저작물에 적용된 이용허락조건을 명확하게 나타내어야 합니다.
- 저작권자로부터 별도의 허가를 받으면 이러한 조건들은 적용되지 않습니다.

저작권법에 따른 이용자의 권리는 위의 내용에 의하여 영향을 받지 않습니다.

이것은 [이용허락규약\(Legal Code\)](#)을 이해하기 쉽게 요약한 것입니다.

[Disclaimer](#)

Master's Thesis

Synthesis and Reactivity of Xantphos Complexes of
Nickel for the Nickel-Catalyzed Azide–Alkyne
Cycloaddition

Jaegwan Kim

Department of Chemistry

Graduate School of UNIST

2020

Synthesis and Reactivity of Xantphos Complexes of Nickel for the Nickel-Catalyzed Azide–Alkyne Cycloaddition

Jaegwan Kim

Department of Chemistry

Graduate School of UNIST

Synthesis and Reactivity of Xantphos Complexes
of Nickel for the Nickel-Catalyzed Azide–Alkyne
Cycloaddition

A thesis/dissertation
submitted to the Graduate School of UNIST
in partial fulfillment of the
requirements for the degree of
Master of Science

Jaegwan Kim

12/11/2019 of submission

Approved by



Advisor

Jan-Uwe Rohde

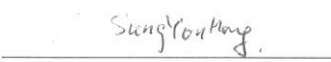
Synthesis and Reactivity of Xantphos Complexes
of Nickel for the Nickel-Catalyzed Azide–Alkyne
Cycloaddition


Jaegwan Kim

This certifies that the thesis/dissertation of Jaegwan Kim is approved.

12/11/2019 of submission



Advisor: Prof. Jan-Uwe Rohde

Prof. Sung You Hong: Thesis Committee Member

Prof. Jung-Min Kee: Thesis Committee Member

Acknowledgement

I appreciate to my advisor prof. Jae-Uwe Rohde, for all of his supports, advice and assistance throughout my graduate course.

I also appreciate to members of the Rohde group, especially M.S. Jungha Lee, for their supports, advice and assistance.

I would like to thank prof. Sung You Hong, Dr. Woo Gyum Kim and Seo Young Jung for collaboration work with them.

I appreciate to my entire family for their support and encouragement.

Abstract

The transition-metal-catalyzed cycloaddition of organoazides and alkynes is an attractive method for the synthesis of 1,2,3-triazoles, because it offers high atom economy and high yields. The recently discovered Ni-catalyzed azide-alkyne cycloaddition (NiAAC), which employs $[\text{NiCp}_2]$ and 4,5-bis(diphenylphosphino)-9,9-dimethylxanthene (xantphos), allows the synthesis of 1,5-disubstituted 1,2,3-triazoles with high regioselectivity as well as the synthesis of 1,4,5-trisubstituted 1,2,3-triazoles. In comparison with other methods, this reaction can be performed at ambient temperature and not only in organic solvents and under inert conditions but also in H_2O and air. In this work, xantphos complexes of Ni were synthesized and their reactivity was investigated to gain insights into the identity and formation of the catalytically active species as well as the possible mechanism of this reaction.

The air-sensitive alkyne complexes $[\text{Ni}(\text{xantphos})(\text{PhCCR})]$ (where $\text{R} = \text{H}$ or Ph) were synthesized by reaction of $[\text{Ni}(\text{cod})_2]$ (where $\text{cod} = 1,5\text{-cyclooctadiene}$) with xantphos and the respective alkyne. The complexes were characterized by NMR spectroscopy, elemental analysis and mass spectrometry. The complex $[\text{Ni}(\text{xantphos})\text{Cl}_2]$ was synthesized by reaction of $\text{NiCl}_2 \cdot 6\text{H}_2\text{O}$ with xantphos and characterized by ESI mass spectrometry and elemental analysis.

The catalytic activity of these complexes was explored in reactions of benzylazide with the terminal alkyne phenylethyne and the internal alkyne diphenylethyne in toluene under inert conditions. In case of the terminal alkyne, the Ni^0 complexes $[\text{Ni}(\text{xantphos})_2]$ and $[\text{Ni}(\text{xantphos})(\text{PhCCR})]$ produced isolated yields of over 85 % of 1,5-disubstituted 1,2,3-triazole and ≤ 6 % of 1,4-disubstituted 1,2,3-triazole, similar to yields obtained with the $[\text{NiCp}_2]/\text{xantphos}$ system. When the internal alkyne was used, yields of over 85 % of 1,4,5-trisubstituted 1,2,3-triazole were obtained. In contrast, $[\text{Ni}(\text{cod})_2]$ and $[\text{Ni}(\text{xantphos})\text{Cl}_2]$ gave at best poor yields (< 20 %) but in most cases only trace amounts of the 1,2,3-triazoles. The catalytic activity of $[\text{Ni}(\text{xantphos})_2]$ was preserved in air with either toluene or H_2O as the solvent in the presence of the additive Cs_2CO_3 , which is also required in case of the $[\text{NiCp}_2]/\text{xantphos}$ system.

Furthermore, the catalytic reactions of $[\text{Ni}(\text{xantphos})_2]$ and $[\text{Ni}(\text{xantphos})(\text{PhCCH})]$ were investigated by NMR spectroscopy. Both complexes exhibit high catalytic activity even with a lower catalyst loading of only 1 mol %. These studies showed that $[\text{Ni}(\text{xantphos})(\text{PhCCH})]$ is present during the catalytic reaction in both cases. Reactions of these complexes with individual substrates revealed that $[\text{Ni}(\text{xantphos})_2]$ reacts with phenylethyne to afford $[\text{Ni}(\text{xantphos})(\text{PhCCH})]$ under release of one of the two xantphos ligands and that the alkyne complex rapidly reacts with benzylazide to form 1,5-disubstituted 1,2,3-triazole. Moreover, $[\text{Ni}(\text{xantphos})_2]$ also reacts with benzylazide under release of xantphos, but this reaction is slower than that with phenylethyne. A systematic study of reactions of

[NiCp₂] with xantphos, phenylethyne and benzylazide in varying stoichiometric ratios indicated the formation of [Ni(xantphos)₂] and [Ni(xantphos)(PhCCH)]. These results suggest that the alkyne complex may be formed in the [NiCp₂]/xantphos system and may act as the catalytically active species.

Table of Contents

Acknowledgement	i
Abstract	ii
List of Figures	v
List of Schemes	vii
List of Tables	ix

Chapters

1. Introduction	1
2. Background	2
3. Synthesis and Characterization of Xantphos Complexes of Nickel	8
3.1 Introduction	8
3.2 Experimental Section	9
3.2.1 Materials and Methods	9
3.2.2 Preparation of Xantphos Complexes of Nickel	9
3.3 Results and Discussion	12
3.4 Conclusion	16
4. Investigation of the Azide–Alkyne Cycloaddition with Nickel Complexes	21
4.1 Introduction	21
4.2 Experimental Section	22
4.2.1 Materials and Methods	22
4.2.2 Procedure for the Nickel-Catalyzed Azide–Alkyne Cycloaddition	22
4.2.3 Preparation of Reaction Solutions for NMR Spectroscopy	22
4.3 Results and Discussion	24
4.3.1 Catalytic Studies	24
4.3.2 NMR Spectroscopic Studies	26
4.4 Conclusion	36
5. Summary and Conclusion	44
6. References	46

List of Figures

Figure 1. Time course (^1H NMR, 400 MHz, 25 $^\circ\text{C}$) of the reaction of 100 mM 2 (open circles) with 1.2 equiv of 1a (open triangles) in the presence of 1 mM (1 mol %) 6 in benzene- d_6 , producing 3a (solid circles).	27
Figure 2. Time course (^1H NMR, 400 MHz, 25 $^\circ\text{C}$) of the reaction of 100 mM 2 (open circles) with 1.2 equiv of 1a (open triangles) in the presence of 1 mM (1 mol %) 7a in benzene- d_6 , producing 3a (solid circles).	27
Figure 3. Time courses (^1H NMR, 400 MHz, 25 $^\circ\text{C}$) of the reactions of 1 mM 6 with a) 10 equiv of 1a and b) 10 equiv of 2 in benzene- d_6 , showing the formation of 7a [a) solid triangles] and the release of xantphos [a) solid diamonds and b) open diamonds].	30
Figure 4. Time course (^1H NMR, 400 MHz, 25 $^\circ\text{C}$) of the reaction of 200 mM 2 with 1.2 equiv of 1a in the presence of 20 mM (10 mol %) NiCp $_2$ and xantphos in benzene- d_6 . Top: Conversion of 1a (open triangles) and 2 (open circles) into 3a (solid circles). Bottom: xantphos (solid diamonds).	33
Figure 5. Time course (^1H NMR, 400 MHz, 25 $^\circ\text{C}$) of the reaction of 10 mM NiCp $_2$ with 10 equiv of xantphos in benzene- d_6 , showing the formation of 6 (solid squares) and the change in the concentration of xantphos (solid diamonds).	34
Figure 6. Time course (^1H NMR, 400 MHz, 25 $^\circ\text{C}$) of the reaction of 10 mM NiCp $_2$ with 3 equiv of xantphos, 2 equiv of 1a and 1 equiv of 2 in benzene- d_6 , showing the formation of 3a (solid circles) and 7a (solid triangles) and the change in the concentration of xantphos (solid diamonds).	35
Figure S1. ^1H NMR spectrum of 7a in benzene- d_6 (400 MHz, 25 $^\circ\text{C}$).	17
Figure S2. ^{31}P NMR spectrum of 7a in benzene- d_6 (162 MHz, 25 $^\circ\text{C}$).	17
Figure S3. ^1H NMR spectrum of 7b in benzene- d_6 (400 MHz, 25 $^\circ\text{C}$).	18
Figure S4. ^{31}P NMR spectrum of 7b in benzene- d_6 (162 MHz, 25 $^\circ\text{C}$).	18
Figure S5. ^1H NMR spectrum of 7b in tetrahydrofuran- d_8 (400 MHz, 25 $^\circ\text{C}$).	18
Figure S6. ^{13}C NMR spectrum of 7b in tetrahydrofuran- d_8 (101 MHz, 25 $^\circ\text{C}$).	19
Figure S7. ^{31}P NMR spectrum of 7b in tetrahydrofuran- d_8 (162 MHz, 25 $^\circ\text{C}$).	20
Figure S8. ^1H NMR spectrum of the product solution ($t = 51$ min) of the reaction of 100 mM 2 with 1.2 equiv of 1a in the presence of 1 mM (1 mol %) 6 in benzene- d_6 (400 MHz, 25 $^\circ\text{C}$).	37
Figure S9. ^1H NMR spectrum of the product solution ($t = 19$ min) of the reaction of 100 mM 2 with 1.2 equiv of 1a in the presence of 1 mM (1 mol %) 7a in benzene- d_6 (400 MHz, 25 $^\circ\text{C}$).	37
Figure S10. NMR spectra of the product solution ($t = 15$ min) of the reaction of 100 mM 2 with 1.2 equiv of 1a in the presence of 10 mM (10 mol %) 7a in benzene- d_6 . Top: ^1H NMR spectrum (400 MHz, 25 $^\circ\text{C}$). Bottom: ^{31}P NMR spectrum (162 MHz, 25 $^\circ\text{C}$).	38

Figure S11. NMR spectra of the product solution ($t = 115$ min) of the reaction of 1 mM **6** with 10 equiv of **1a** in benzene- d_6 . Top: ^1H NMR spectrum (400 MHz, 25 °C). Bottom: ^{31}P NMR spectrum (162 MHz, 25 °C). 39

Figure S12. NMR spectra of the product solution ($t = 4$ min) of the reaction of 10 mM **7a** with 10 equiv of **2** in benzene- d_6 . Top: ^1H NMR spectrum (400 MHz, 25 °C). Bottom: ^{31}P NMR spectrum (162 MHz, 25 °C). 40

Figure S13. NMR spectra of the product solution ($t = 6$ h) of the reaction of 200 mM **2** with 1.2 equiv of **1a** in the presence of 20 mM (10 mol %) NiCp_2 and xantphos in benzene- d_6 . Top: ^1H NMR spectrum (400 MHz, 25 °C). Bottom: ^{31}P NMR spectrum (162 MHz, 25 °C). 41

Figure S14. NMR spectra of the product solution ($t = 48$ h) of the reaction of 10 mM NiCp_2 with 10 equiv of xantphos in benzene- d_6 . Top: ^1H NMR spectrum (400 MHz, 25 °C). Bottom: ^{31}P NMR spectrum (162 MHz, 25 °C). 42

Figure S15. NMR spectra of the product solution ($t = 48$ h) of the reaction of 10 mM NiCp_2 with 3 equiv of xantphos, 2 equiv of **1a** and 1 equiv of **2** in benzene- d_6 . Top: ^1H NMR spectrum (400 MHz, 25 °C). Bottom: ^{31}P NMR spectrum (162 MHz, 25 °C). 43

List of Schemes

Scheme 1. Thermal Azide–Alkyne Cycloaddition	2
Scheme 2. CuAAC to Produce 1,4-Disubstituted 1,2,3-Triazoles	2
Scheme 3. Example of Very Fast CuAAC Reactions	3
Scheme 4. CuAAC to Produce 1,4,5-Trisubstituted 1,2,3-Triazoles	3
Scheme 5. Initially Proposed Mononuclear Mechanism of CuAAC by Fokin, Sharpless and Co-workers	4
Scheme 6. Dinuclear Mechanism of CuAAC (X is bridging ligand)	4
Scheme 7. RuAAC to Produce 1,5-Disubstituted 1,2,3-Triazole and 1,4,5-Trisubstituted 1,2,3-Triazoles	5
Scheme 8. Proposed Mechanism of RuAAC	5
Scheme 9. Synthesis of 1,5-Disubstituted and 1,4,5-Trisubstituted 1,2,3-Triazoles by the NiAAC	6
Scheme 10. Synthesis of Complex 6	12
Scheme 11. Synthesis of Alkyne Complex 7b	13
Scheme 12. Synthesis of Alkyne Complex 7a	14
Scheme 13. Reactivity of 6 toward Alkynes 1a and 1b	14
Scheme 14. Synthesis of Complex 8	15
Scheme 15. Reaction of 6 with 1a and 2	28
Scheme 16. Reaction of 7a with 1a and 2	29

Scheme 17. Production of Triazole **3a** from Reaction of **7a** with **2** 30

Scheme 18. Proposed Mechanism for the NiAAC Using **6** 31

List of Tables

Table 1. Catalytic Activity of Ni Complexes in the Alkyne–Azide Cycloaddition..... 25

Table 2. Catalytic Activity of [NiCp₂]/Xantphos and **6** in the Alkyne–Azide Cycloaddition in Air · 26

Chapter 1

Introduction

This thesis covers the synthesis and characterization of xantphos complexes of Ni and the investigation of the azide–alkyne cycloaddition (AAC) with the Ni complexes. In the literature, it has been reported that click chemistry can give high atom economy and high yields. The AAC has been widely studied. As a result, synthetic methods to form 1,4-disubstituted 1,2,3-triazoles by Cu-catalyzed AAC (CuAAC) and 1,5-disubstituted 1,2,3-triazoles by Ru-catalyzed AAC (RuAAC) were revealed. Recently, a Ni-catalyzed version (NiAAC) was reported to produce 1,5-disubstituted 1,2,3-triazoles. In comparison with the other methods, this reaction can be performed at ambient temperature and not only in organic solvents and under inert conditions but also in H₂O and air. Moreover, it can be applied to a wide range of substrates. In addition, the NiAAC can be used to give 1,4,5-trisubstituted 1,2,3-triazole, akin to the CuAAC and RuAAC. Studies with well-defined xantphos complexes of Ni may help in the identification of the catalytic active species and the elucidation of the mechanism of this reaction. Results presented in this thesis show that xantphos complexes of Ni can catalyze the AAC, and various NMR spectroscopic experiments provide clues for the mechanism of the reaction.

A brief overview of click chemistry, the AAC and transition-metal catalyzed reactions will be presented in Chapter 2. Click reactions typically entail overall joining of molecular pieces like the two pieces of a seat belt buckle. Examples of AAC will be discussed. Moreover, transition-metal-catalyzed AAC will be presented as well as their theoretical background. These examples will serve as a useful foundation for exploring the synthesis and reactivity of xantphos complexes of Ni for the NiAAC.

The synthesis and characterization of four xantphos complexes of Ni will be described in Chapter 3, as these complexes may be candidates of catalysts for this reaction. These include three complexes of Ni⁰ and one of Ni^{II}. The characterization of the Ni⁰ complexes by ¹H and ³¹P NMR spectroscopy provides the basis for the spectroscopic investigation of reactions of these complexes.

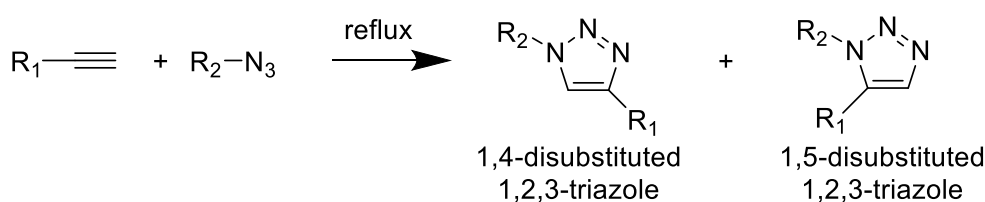
Chapter 4 will focus on the investigation of the AAC with the Ni complexes. For this purpose, the catalytic activity of these complexes was examined in reactions of benzylazide with a terminal and an internal alkyne in toluene. To gain insights into the mechanism of the NiAAC, catalytic and stoichiometric reactions of two Ni⁰ complexes were studied by NMR spectroscopy. Finally, reactions of [NiCp₂] with xantphos were investigated to probe the formation of possible catalytically active species. The relevance of the xantphos complexes to the original [NiCp₂]/xantphos system will be described.

Chapter 2

Background

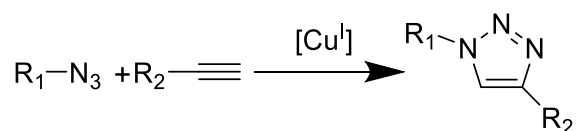
The cycloaddition of azides and alkynes is a representative reaction of click chemistry. The reaction has strength in high atom economy and high yield. The 1,3-cycloaddition of organic azides and alkynes to synthesize 1,2,3-triazoles was first reported by Michael.¹ However, the lack of knowledge of 1,2,3-triazoles discouraged additional investigation of the chemistry. Studies to promote 1,2,3-triazole formation were actually started in the 1960s. The 1,3-dipolar cycloaddition of azides and alkynes to synthesis 1,2,3-triazoles was widely studied by Huisgen (Scheme 1).^{2,3} However, because of the high activation barrier of the reaction, the reaction is slow and unable to control regioselectivity.⁴

Scheme 1. Thermal Azide–Alkyne Cycloaddition²



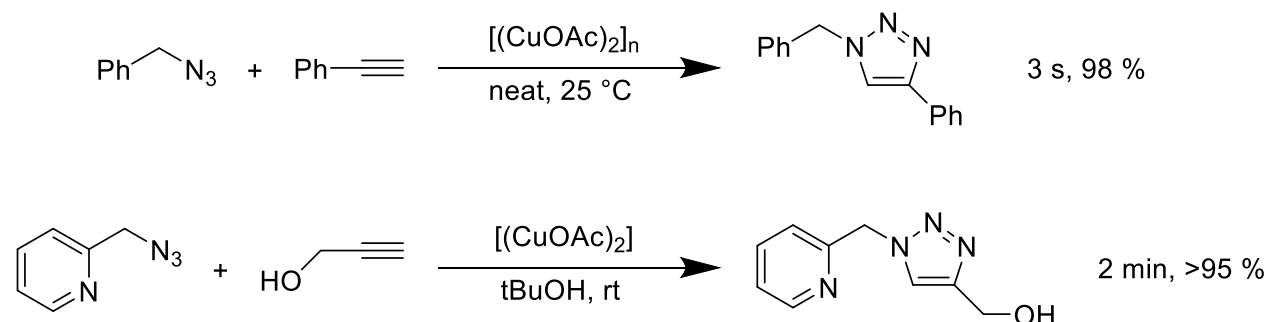
To overcome the limitations, transition metal catalysts were studied. The first catalysts that were found to work as catalysts were Cu catalysts. In the early 2000s, Meldal and co-workers reported a Cu-catalyzed azide–alkyne cycloaddition (Scheme 2).^{5,6} The catalysts successfully worked under mild conditions with high yields. Fokin, Sharpless, and co-workers reported a Cu^I catalyst that was produced in situ by reduction of a Cu^{II} salt.⁷ These catalysts successfully produced 1,4-disubstituted 1,2,3-triazoles in high yield and regioselectivity.

Scheme 2. CuAAC to Produce 1,4-Disubstituted 1,2,3-Triazoles^{6,7}

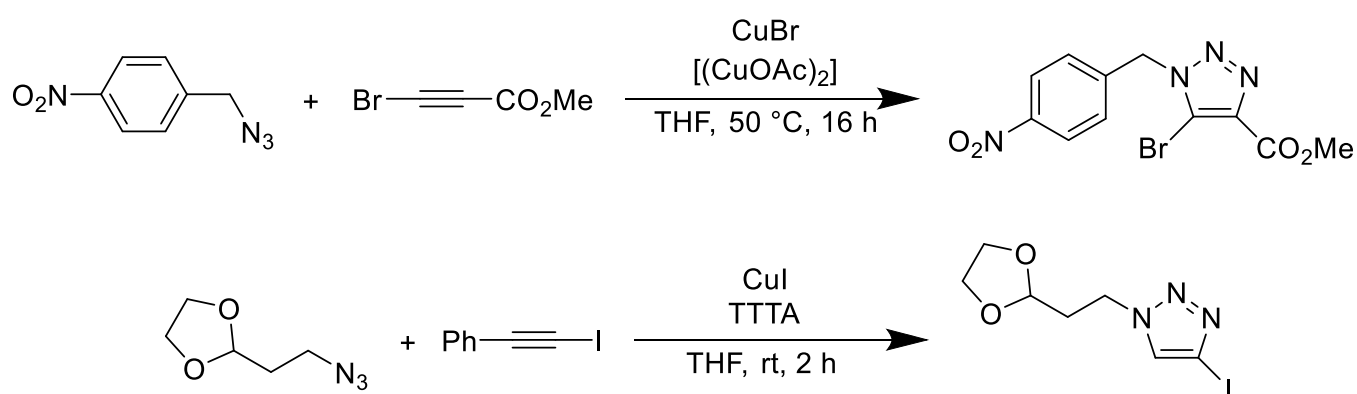


Since the initial investigations, efforts to improve the reactions were continued. Various kinds of substrates and Cu catalyst were studied. In some cases, very short reaction times were achieved, even down to 3 s at 25 °C. Also, some of the Cu catalysts produced 1,4,5-trisubstituted 1,2,3-triazoles. As shown in Schemes 3 and 4, various kinds of Cu salts were used to assist the reaction.

Scheme 3. Example of Very Fast CuAAC Reactions^{8,9}



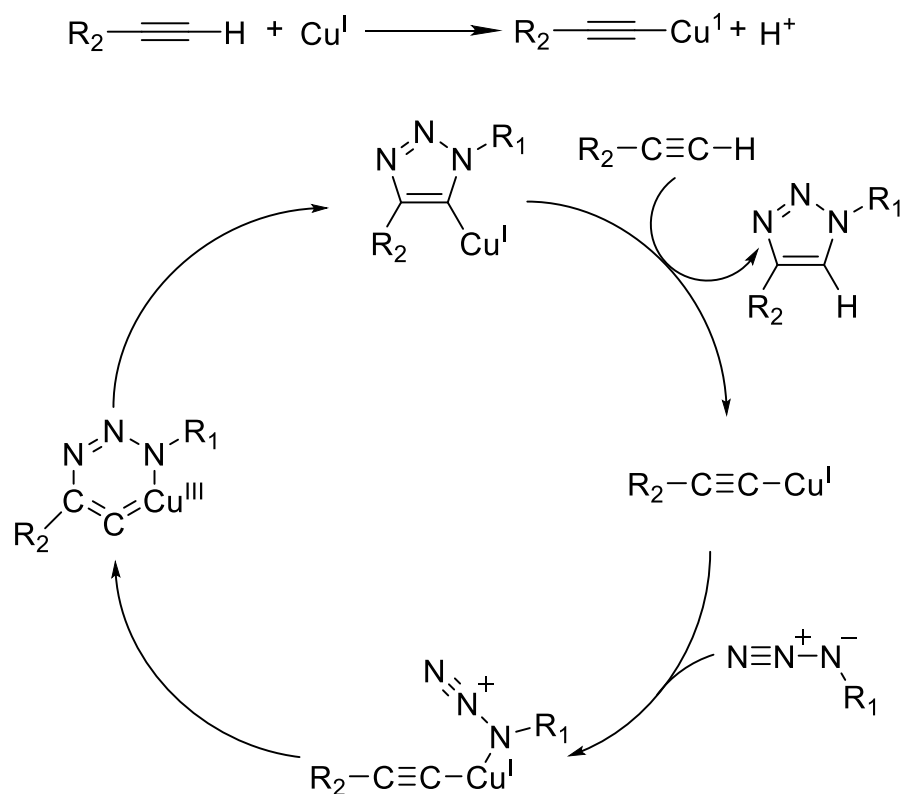
Scheme 4. CuAAC to Produce 1,4,5-Trisubstituted 1,2,3-Triazoles^{4,10}



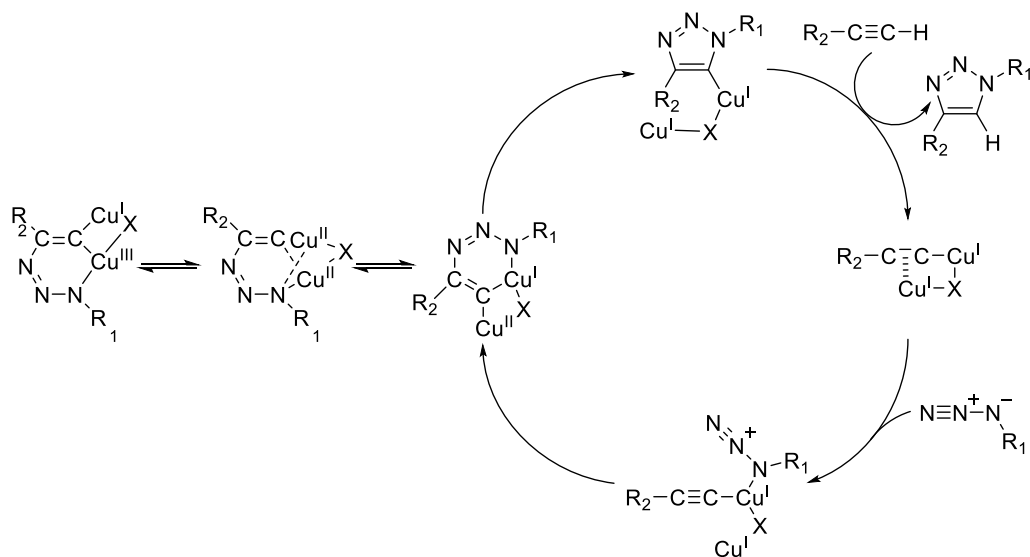
Contemporarily, efforts to discover the reaction mechanism were continued. The initial mechanistic model for catalysis was a mononuclear model proposed by Fokin, Sharpless and co-workers. As shown in Scheme 5, the reaction starts with formation of Cu acetylide and proceeds with addition of organic azide. Then, oxidative coupling occurs so that a C–N bond can be formed and give a metallacycle intermediate. Meanwhile, the Cu^I catalyst is oxidized to Cu^{III}. The second C–N bond is formed with ring contraction to give a Cu triazolide and Cu^{III} is reduced to Cu^I. Lastly, additional alkyne inserts to supply a proton and allow the release of triazole.

However, this model met the limitation that it cannot explain fast formation of the first C–N bond and the metallacycle. Thus, an alternative dinuclear model was proposed. The mechanism is different from the start of the reaction (Scheme 6). Instead of the Cu acetylide, a Cu₂ σ,π-acetylide is the starting point of the reaction. The azide adds to the acetylide complex to form an azide alkyne copper complex. C–N bond formation occurs resulting in formation of a metallacycle. Meanwhile, Cu^I is oxidized to Cu^{III}. The second C–N bond is formed with ring contraction to give Cu triazolide and reduction of Cu^{III} to Cu^I. Lastly, additional alkyne inserts into the complex forming a Cu₂ σ,π-acetylide and releasing 1,2,3-triazole. However, a mechanism to elucidate the reaction of internal alkyne with organic azide to form 1,4,5-trisubstituted 1,2,3-triazole was not established yet.

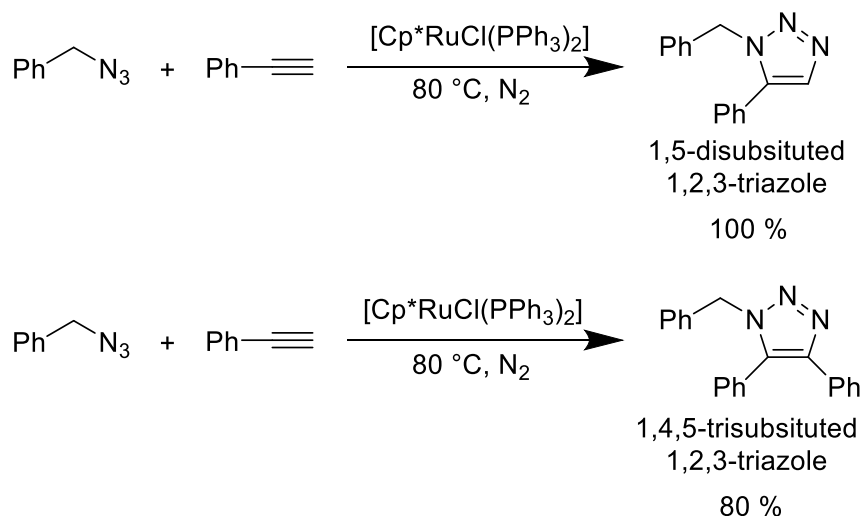
Scheme 5. Initially Proposed Mononuclear Mechanism of CuAAC by Fokin, Sharpless and Co-workers⁷



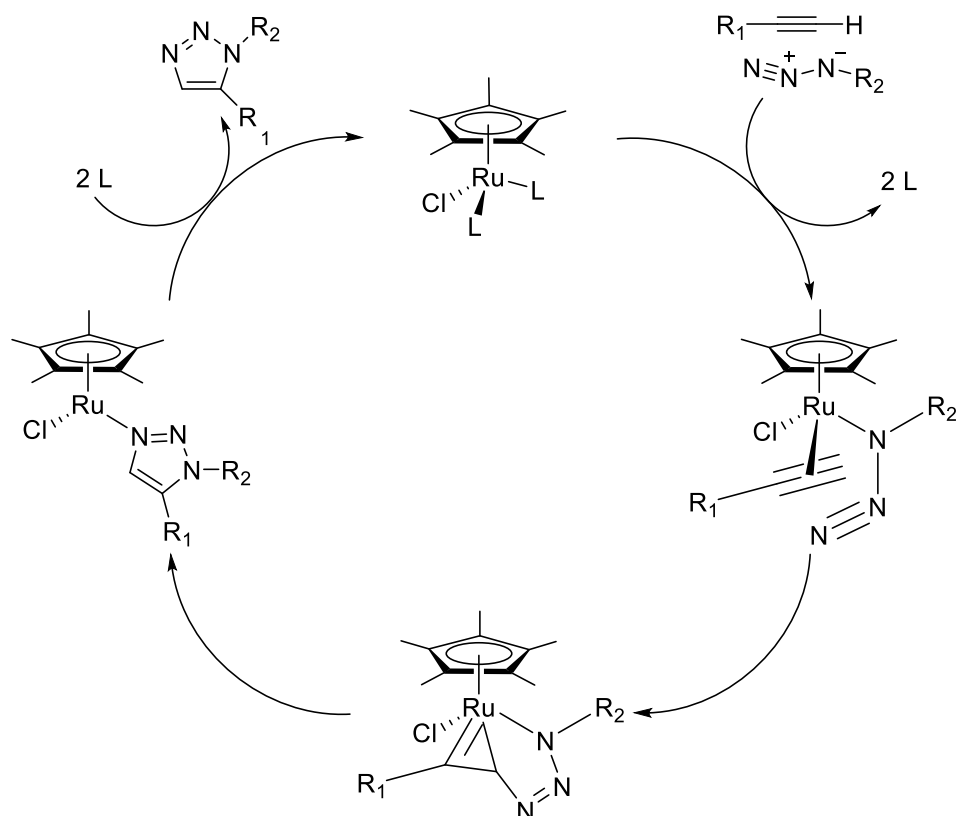
Scheme 6. Dinuclear Mechanism of CuAAC (X is bridging ligand)¹⁰



Scheme 7. RuAAC to Produce 1,5-Disubstituted 1,2,3-Triazole and 1,4,5-Trisubstituted 1,2,3-Triazoles¹¹



Scheme 8. Proposed Mechanism of RuAAC¹²



Although Cu catalysts were successful in the synthesis of 1,4-disubstituted 1,2,3-triazole formation, they were not suitable catalysts to produce 1,5-disubstituted 1,2,3-triazoles. The first transition-metal catalyzed azide–alkyne cycloaddition to synthesize 1,5-disubstituted 1,2,3-triazole was reported in 2005. Fokin and co-workers presented Ru^{II} catalysts that produced the 1,2,3-triazoles in high yield

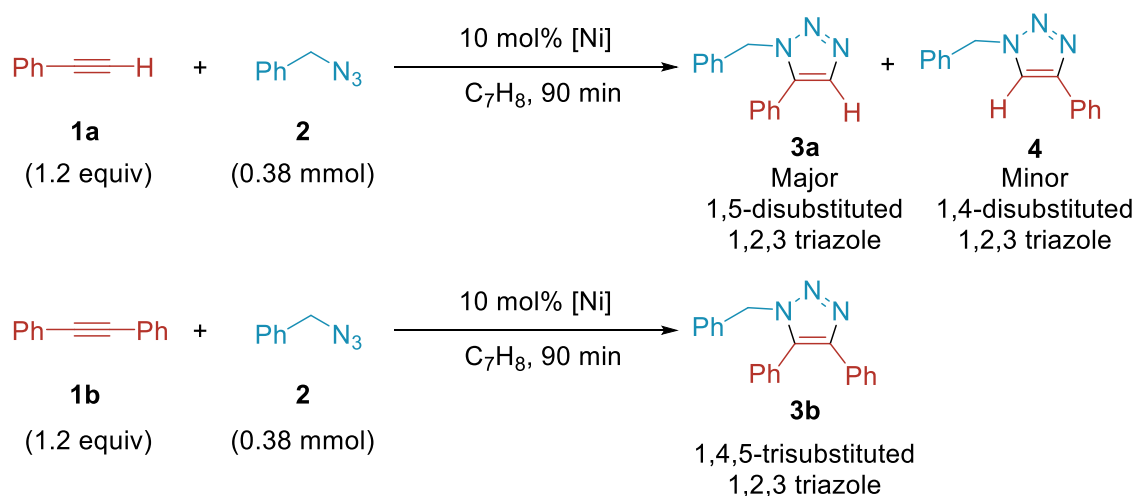
and regioselectivity (Scheme 7).¹¹ The catalysts gave 1,2,3-triazoles from organic azides and alkynes with a broad range of functional groups. The RuAAC could also be applied to yield 1,4,5-trisubstituted 1,2,3-triazoles. In the synthesis of 1,4,5-trisubstituted 1,2,3-triazoles, it could also be applied to various functional groups in yields of 63–97 %.¹²

Contemporarily, efforts to discover reaction mechanism were continued. In 2008, Fokin and co-workers reported that pentamethylcyclopentadienyl (C_5Me_5 or Cp^*) complexes of Ru^{II} exclusively produced 1,5-disubstituted 1,2,3-triazoles. Other complexes of Ru^{II} were not able to catalyze the AAC. Also, $[CpRuCl(PPh_3)_2]$ catalyst gain low yield.¹² Thus, Cp^* complexes of Ru^{II} were proposed as active catalyst. Based on the experimental data and calculations, a mechanism was proposed. As shown in Scheme 8, the substitution of supporting ligands and azide and alkyne occurs. Due to steric effect of the Cp^* ligand, the orientation of the two substrates was fixed. The first C–N bond forms to give a metallacycle. Ring contraction follows to afford a triazolide complex of Ru. As a result, substitution of the supporting ligands occurs resulting in release of 1,5-disubstituted 1,2,3-triazole.¹² However, there were limitations of RuAAC in that it requires elevated temperatures and inert conditions.

Recently, a Ni-catalyzed azide–alkyne cycloaddition was reported by Hong and co-workers to form a wide range of 1,5-disubstituted 1,2,3-triazoles with high regioselectivity as well as 1,4,5-trisubstituted 1,2,3-triazoles. This reaction employs $[NiCp_2]$ and 4,5-bis(diphenylphosphino)-9,9-dimethylxanthene (xantphos). In comparison with the other methods (CuAAC and RuAAC), this reaction can be performed at ambient temperature and not only in organic solvents and under inert conditions but also in H_2O and air.

Scheme 9. Synthesis of 1,5-Disubstituted and 1,4,5-Trisubstituted 1,2,3-Triazoles by the NiAAC

13



Initial efforts to identify the active catalyst in the system were revealed the presence of Ni^{I} and Ni^0 species. In the reaction of $[\text{NiCp}_2]$ with xantphos, a Ni^{I} species, presumably $[\text{NiCp}(\text{xantphos})]$ (**5**), was detected by EPR spectroscopy, and mass spectrometry suggested the presence of $[\text{NiCp}(\text{xantphos})]^+$ and $[\text{Ni}(\text{xantphos})_2]$ (**6**).

In this thesis, relevant xantphos complexes of Ni were synthesized and their reactivity was investigated to gain insights into the identity and formation of the catalytically active species as well as the possible mechanism of this reaction.

Chapter 3

Synthesis and Characterization of Xantphos Complexes of Nickel

3.1 Introduction

In this chapter, the synthesis of four xantphos complexes of Ni will be described. In particular, these include the tetrakis(phosphine) complex $[\text{Ni}(\text{xantphos})_2]$ (**6**), the two alkyne complexes $[\text{Ni}(\text{xantphos})(\text{PhCCH})]$ (**7a**) and $[\text{Ni}(\text{xantphos})(\text{PhCCPh})]$ (**7b**) and the dichloride complex $[\text{Ni}(\text{xantphos})\text{Cl}_2]$ (**8**). These complexes are potential catalyst candidates for the NiAAC and their reactivity will be described in Chapter 4.

The method for synthesizing the air-sensitive Ni^0 complexes entails ligand substitution reactions of $[\text{Ni}(\text{cod})_2]$ with xantphos or alkynes in appropriate molar ratios under an N_2 atmosphere. The Ni^{II} complex was synthesized by the reaction of $\text{NiCl}_2 \cdot 6\text{H}_2\text{O}$ with xantphos.

Characterization of the complexes by elemental analysis, multinuclear (^1H , ^{13}C and ^{31}P) NMR spectroscopy and mass spectrometry was conducted in order to confirm the identity of the complexes synthesized.

3.2 Experimental Section

3.2.1 Materials and Methods

Materials. All reagents and solvents were purchased from commercial sources and were used as received, unless noted otherwise. Diethyl ether, toluene and tetrahydrofuran were deoxygenated by sparging with N₂ and purified by passage through two packed columns of molecular sieves under an N₂ pressure (MBraun solvent purification system). *n*-Pentane was dried over Na and distilled under N₂ prior to use.¹⁴ [Ni(cod)₂] and NiCl₂·6H₂O, ReagentPlus grade, were purchased from Sigma-Aldrich and xantphos, >98.0 %, was purchased from Tokyo Chemical Industry Co. Preparation and handling of air- and moisture-sensitive materials were carried out under an inert gas atmosphere by using either standard Schlenk and vacuum line techniques or a glovebox. The complexes [Ni(xantphos)₂] (**6**), [Ni(xantphos)(PhCCH)] (**7a**) and [Ni(xantphos)(PhCCPh)] (**7b**) are air-sensitive and were therefore prepared and handled in an N₂ atmosphere. Complex [Ni(xantphos)Cl₂] (**8**) was prepared (excluding work-up) in an N₂ atmosphere but handled in air.

Physical Methods. NMR spectra were recorded on a Bruker Avance III 400 spectrometer at ambient temperature. ¹H, ¹³C and ³¹P chemical shifts are reported in parts per million (ppm) and were referenced to residual solvent peaks (for ¹H and ¹³C NMR spectra) or an external standard [triphenyl phosphate (0.0485 M in acetone-*d*₆, −17.57 ppm) for ³¹P NMR spectra]. Electrospray ionization mass spectral (ESI MS) data were acquired on a quadrupole ion trap Bruker HCT Basic System mass spectrometer or on a time-of-flight JEOL AccuTOF DART 4G+ mass spectrometer. Electron impact ionization mass spectral (EIMS) data were acquired on a tandem triple quadrupole Bruker 320-MS mass spectrometer (equipped with a direct insertion probe). Elemental analysis was performed using a Leco TruSpec Micro analyzer (combustion analysis).

3.2.2 Preparation of Xantphos Complexes of Nickel

[Ni(xantphos)₂] (6**).** This complex was synthesized according to a procedure to be reported elsewhere.¹⁵ A solution of 0.55 g (2.00 mmol) of [Ni(cod)₂] in 20 ml of toluene was added to 2.315 g (4.00 mmol) of xantphos, and the resulting red suspension was stirred for 4 h. The reaction mixture gradually turned orange within 30 min. After addition of 8 ml of diethyl ether to the suspension, the orange precipitate was separated by filtration, washed with diethyl ether and dried *in vacuo*. Yield: 2.37 g (97 %). ¹H NMR (400 MHz, C₆D₆, δ): 7.69–7.36 (br m, Ar H), 7.16–6.74 (br m, Ar H; these signals partially overlap with the residual solvent peak), 6.63–6.45 (br m, Ar H), 6.37–6.24 (br m, Ar H), 1.44 (s, CH₃). ³¹P NMR (162 MHz, C₆D₆, δ): 10.0–9.4 (m, PAr₃) and 8.9–8.2 (m, PAr₃).

[Ni(xantphos)(PhCCH)] (7a**).** **Method A.** A solution of 174 mg (0.300 mmol) of xantphos in 6 ml of toluene was added to a solution of 82.6 mg (0.300 mmol) of [Ni(cod)₂] and 107 mg (0.588 mmol) of

diphenylethyne (98 %; **1b**) in 4 ml of toluene. The reaction mixture was stirred for 4 h. The red solution turned into an orange suspension within 10 min, which became yellow after 30 min. After addition of 3 ml of *n*-pentane to the suspension, the yellow precipitate was separated by filtration and washed with *n*-pentane. Next, 6 ml of tetrahydrofuran and 336 μ l (31.3 mg, 3.00 mmol) of phenylethyne (**1a**) were added to the solid. The reaction mixture was stirred for 4 h. Then, 6 ml of *n*-pentane was added to precipitate unreacted **7b**. The mixture was filtered and the filtrate was evaporated to dryness. The residue was recrystallized from diethyl ether by preparing a concentrated solution at room temperature and storing it at $-30\text{ }^{\circ}\text{C}$. Yield: 161 mg (73 %). Anal. Calcd for $\text{C}_{47}\text{H}_{38}\text{NiO}_2\text{P}_2$ (**7a** + O): C, 74.72; H, 5.07. Found: C, 74.69; H, 5.13. (Due to the air sensitivity of the product, it may have been oxidized.) ^1H NMR (400 MHz, C_6D_6 , δ): 7.71–7.57 (m, 8 H), 7.11–6.97 (m, 10 H), 6.95–6.62 (m, 14 H), 1.34 (s, 6 H, CH_3). $^{31}\text{P}\{^1\text{H}\}$ NMR (162 MHz, C_6D_6 , δ): 23.0 and 21.8 (dd, $J = 190\text{ Hz}$, $J = 20\text{ Hz}$, PAr_3). ESI(+)MS (solvent, thf; supporting solvent, EtOH) m/z calcd for $\text{C}_{47}\text{H}_{38}\text{NiOP}_2$, 738.2; found, 737.3 ($\{\text{M} - \text{H}^+\}^+$), 617.3 ($\{\text{xantphos} + \text{K}\}^+$), 633.3 ($\{\text{xantphos} + \text{O} + \text{K}\}^+$).

Method B. A solution of 116 mg (0.200 mmol) of xantphos and 27.5 mg (0.100 mmol) of $[\text{Ni}(\text{cod})_2]$ in 5 ml of toluene was stirred for 4 h. The resulting red suspension gradually turned orange. Next, 11.2 μ l (10.4 mg, 0.100 mmol) of **1a** was added and the reaction mixture was stirred for 4 h, during which time the orange suspension became a solution. To convert free xantphos into **6**, a solution of 13.6 mg (0.0494 mmol) of $[\text{Ni}(\text{cod})_2]$ in 5 ml of tetrahydrofuran was added. The resulting mixture immediately turned into a brown suspension and was stirred for 4 h. After addition of 3 ml of diethyl ether, the suspension was filtered and the filtrate was evaporated to dryness. The residue was recrystallized from diethyl ether by preparing a concentrated solution at room temperature and storing it at $-30\text{ }^{\circ}\text{C}$. Yield: 8.0 mg (11 %). The ^1H and ^{31}P NMR spectra of this batch were identical to those of the product obtained from Method A.

$[\text{Ni}(\text{xantphos})(\text{PhCCPh})]$ (7b**).** While the synthesis of this compound was reported previously,^{16a} two modified procedures were utilized in this work. **Method A.** A solution of 274 mg (1.51 mmol) of **1b** (98 %) and 82.5 mg (0.300 mmol) of $[\text{Ni}(\text{cod})_2]$ in 8 ml of toluene was stirred for 5 min. A solution of 174 mg (0.300 mmol) of xantphos in 4 ml of toluene was added and the resulting solution was stirred for 4 h, giving a yellow suspension. After addition of 4 ml of *n*-pentane, the precipitate was separated by filtration and washed with *n*-pentane to yield 234 mg of a yellow solid. The crude product was recrystallized by vapor diffusion of *n*-pentane into a tetrahydrofuran solution. Yield: 162 mg (66 %). Anal. Calcd for $\text{C}_{53}\text{H}_{42}\text{NiOP}_2$: C, 78.05; H, 5.19. Found: C, 77.50; H, 5.01. ^1H NMR (400 MHz, $\text{thf}-d_8$, δ): 7.49 (d, $J = 8\text{ Hz}$, 2 H, Ar H), 7.33 (m, 8 H, Ar H), 7.08 (t, $J = 8\text{ Hz}$, 4 H, Ar H), 6.99 (t, $J = 8\text{ Hz}$, 10 H, Ar H), 6.70–6.61 (m, 10 H, Ar H), 6.41 (t, $J = 4\text{ Hz}$, 2 H, Ar H), 1.63 (s, 6 H, CH_3). $^{13}\text{C}\{^1\text{H}\}$ NMR (101 MHz, $\text{thf}-d_8$, δ): 158.2 (t, $J_{\text{CP}} = 5\text{ Hz}$), 137.7 (t, $J_{\text{CP}} = 6\text{ Hz}$), 136.4 (s), 135.6–135.1 (m),

134.8 (t, $J_{\text{CP}} = 7$ Hz), 131.9 (s), 129.8 (s), 129.4 (s), 129.1 (s), 128.5 (t, $J_{\text{CP}} = 4.5$ Hz), 128.0 (s), 127.8 (s), 126.5 (s), 124.6 (s), 124.2 (s), 37.7 (s, $\text{C}(\text{CH}_3)_2$), 27.2 (s, $\text{C}(\text{CH}_3)_2$). $^{31}\text{P}\{^1\text{H}\}$ NMR (162 MHz, $\text{thf-}d_8$, δ): 22.9 (s, PAr_3). ^1H NMR (400 MHz, C_6D_6 , δ): 7.65 (t, $J = 8.0$ Hz, 8H, Ar H), 7.10–7.01 (m, 6 H, Ar H), 6.95–6.84 (m, 12 H, Ar H), 6.81 (t, $J = 4$ Hz, 6 H, Ar H), 6.72 (t, $J = 8$ Hz, 2 H, Ar H), 6.65 (t, $J = 8$ Hz, 2 H, Ar H), 1.32 (s, 6 H, CH_3). $^{31}\text{P}\{^1\text{H}\}$ NMR (162 MHz, C_6D_6 , δ): 22.3 (s, PAr_3). EIMS (70 eV) m/z : M^{++} calcd for $\text{C}_{53}\text{H}_{42}\text{NiOP}_2$, 814.2; found, 814.4 (M^{++}), 578.4 (xantphos^{++}).

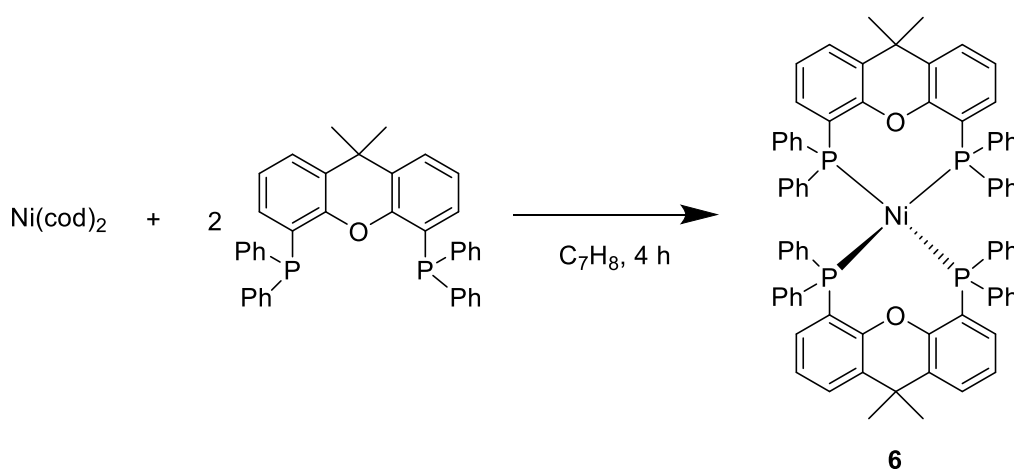
Method B. To a mixture of 174 mg (0.300 mmol) of xantphos and 82.5 mg (0.300 mmol) of $[\text{Ni}(\text{cod})_2]$ in 7 ml of toluene was added a solution of 109 mg (0.599 mmol) of **1b** (98 %) and 46.4 μl (0.464 mg, 0.45 mmol) of benzonitrile in 3 ml of toluene. The reaction mixture was stirred for 4 h. The red solution turned into an orange suspension within 10 min, which became yellow after 30 min. After addition of 4 ml of *n*-pentane, the precipitate was separated by filtration and washed with *n*-pentane to yield 242 mg of a yellow solid. The crude product was recrystallized by vapor diffusion of *n*-pentane into a tetrahydrofuran solution. Yield: 167 mg (68 %). Anal. Calcd for $\text{C}_{53}\text{H}_{42}\text{NiOP}_2$: C, 78.05; H, 5.19. Found: C, 78.05; H, 5.19. ESI(+)MS (solvent, thf ; supporting solvent, EtOH) m/z : $\{\text{M} + \text{Na}\}^+$ calcd for $\text{C}_{53}\text{H}_{42}\text{NiOP}_2$, 837.2; found, 837.3 ($\{\text{M} + \text{Na}\}^+$), 579.3 ($\{\text{xantphos} + \text{H}\}^+$). The ^1H , ^{13}C and ^{31}P NMR spectra of this batch were identical to those of the product obtained from Method A.

$[\text{Ni}(\text{xantphos})\text{Cl}_2]$ (8). In an N_2 atmosphere, 415 mg (2.00 mmol) of $\text{NiCl}_2 \cdot 6\text{H}_2\text{O}$ and 1.18 g (2.00 mmol) of xantphos were suspended in 11 ml of degassed *n*-butanol (99.5 %). The suspension was heated under reflux for 2 h, turning dark violet and eventually gray-violet. After the reaction mixture was allowed to cool down to room temperature, the precipitate was separated by filtration (in air) and washed twice with ethanol, twice with diethyl ether and once with 2:1 diethyl ether–dichloromethane to yield 1.43 g of a gray-violet solid. The crude product was recrystallized by vapor diffusion of diethyl ether into a dichloromethane solution at 4 °C. After three days, the overstanding solution was decanted from the precipitate formed and evaporated to dryness, and the residue was recrystallized once more. The combined fractions were washed with 2:1 diethyl ether–dichloromethane and dried *in vacuo*. Yield: 1.19 g (84 %). Anal. Calcd for $\text{C}_{40}\text{H}_{34}\text{Cl}_4\text{NiOP}_2$ (**8**· CH_2Cl_2): C, 60.57; H, 4.32. Found: C, 60.89; H, 4.24. ESI(+)MS (CH_2Cl_2) m/z : $\{\text{M} - \text{Cl}\}^+$ calcd for $\text{C}_{39}\text{H}_{32}\text{Cl}_2\text{NiOP}_2$, 671.1; found, 671.6.

3.3 Results and Discussion

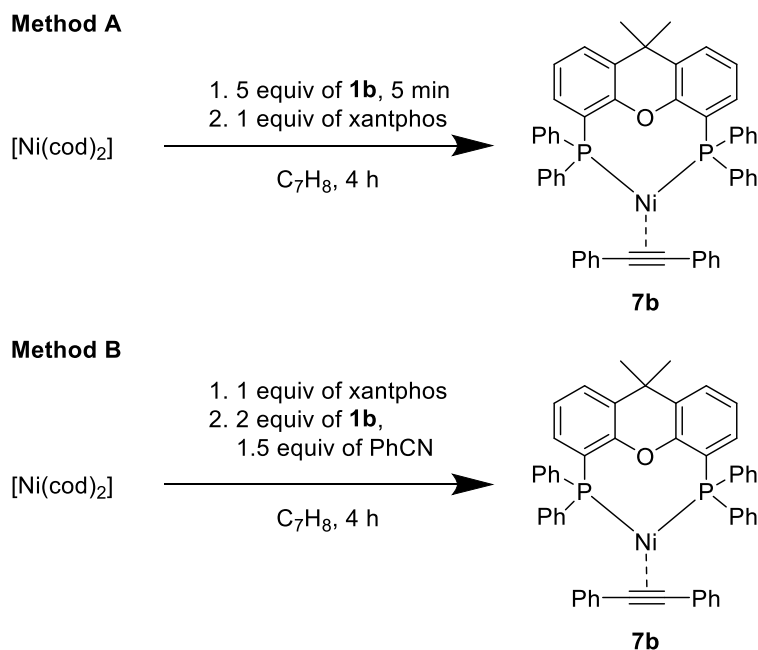
The bis(chelate) complex **6** was synthesized by a substitution reaction of the Ni⁰ precursor [Ni(cod)₂] with the phosphine ligand (Scheme 10), in a similar manner as reported for other tetrakis(phosphine) complexes of Ni.¹⁷ Because of its low solubility, the complex was readily isolated and obtained in nearly quantitative yield. Here, it was characterized by ¹H and ³¹P NMR spectroscopy. The ³¹P NMR spectrum agrees with that previously reported for this complex generated *in situ*.^{16b}

Scheme 10. Synthesis of Complex **6**



To synthesize the alkyne complexes **7a** and **7b**, a method^{16a} reported for the synthesis of a few complexes of internal alkynes, including **7b**, was considered. This method involves the addition of the internal alkyne to a solution of [Ni(cod)₂] and xantphos and employs benzonitrile to catalyze the substitution of the alkyne for one of the two xantphos ligands in **6**, which is commonly formed in solutions of [Ni(cod)₂] and xantphos even when less than two equivalents of xantphos is used.² Therefore, in this work **7b** was initially synthesized following that method with minor modifications (Scheme 11, Method B). Alternatively, **7b** was synthesized by sequential addition of an excess of **1b** and a stoichiometric amount of xantphos to [Ni(cod)₂] (Scheme 11, Method A). Thus, the presence of **1b** can effectively prevent the formation of the bis(chelate) complex **6**, which is consistent with a solution experiment^{16a} mentioned previously. Both methods utilized here gave the complex in good yields after recrystallization and analytically pure form. The ¹H, ¹³C and ³¹P NMR data (thf-*d*₈) are largely consistent with the literature. Here, also data on samples in benzene-*d*₆ were included, which are needed as reference for the reactivity studies (Chapter 4). In addition, **7b** was identified by its molecular ion peak in its EI mass spectrum and by an {M + Na}⁺ ion in its ESI mass spectrum.

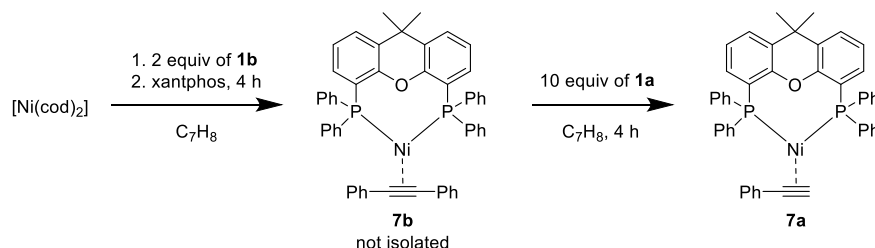
Scheme 11. Synthesis of Alkyne Complex **7b**



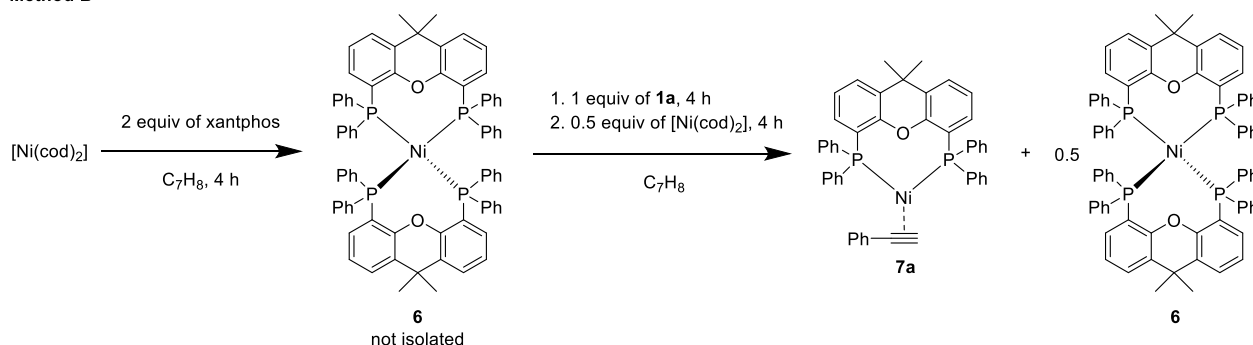
Attempts to synthesize the phenylethyne complex **7a** using either of the two methods described above were not successful. As indicated by ^1H and ^{31}P NMR spectroscopy, the products from reactions with the terminal alkyne **1a** contained free xantphos and impurities that could not be removed. Instead, the new complex **7a** could be cleanly synthesized by substitution of **1a** for the alkyne ligand in **7b** (Scheme 12, Method A). For this purpose, **7b** was prepared and used without purification in the alkyne exchange step. The desired complex of the terminal alkyne was obtained in a good yield after recrystallization.

Scheme 12. Synthesis of Alkyne Complex **7a**

Method A

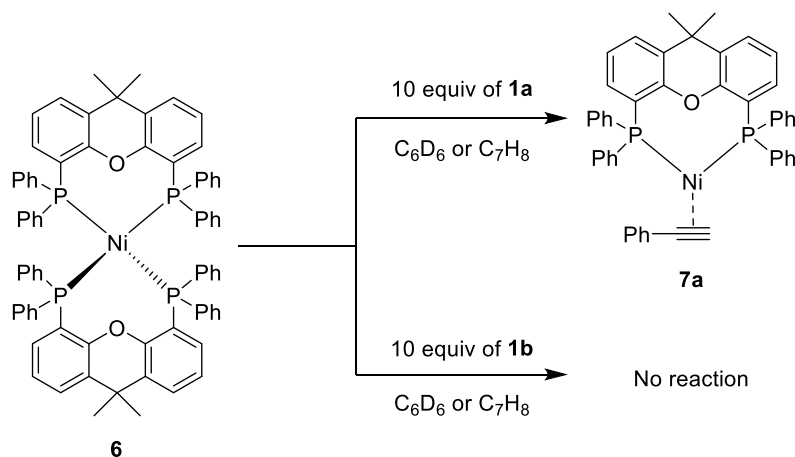


Method B



Interestingly, this complex is also accessible from **6**. While **6** resists ligand exchange with **1b**, it is slowly but quantitatively converted into **7a** and free xantphos upon reaction with **1a** (Scheme 13). Unfortunately, the separation of the desired product from the free phosphine generated in the reaction failed because of an insufficient difference in solubility. However, by addition of half an equivalent of $[\text{Ni}(\text{cod})_2]$, the free phosphine could be converted into **6** (Scheme 12, Method B), which is much less soluble than **7a**. But this method gave **7a** in a much lower yield than did Method A, which therefore is the preferred method. Complex **7a** is soluble in toluene, tetrahydrofuran, diethyl ether and *n*-pentane. For comparison, **7b** is generally less soluble than **7a** and is poorly soluble in diethyl ether and *n*-pentane.

Scheme 13. Reactivity of **6** toward Alkynes **1a** and **1b**

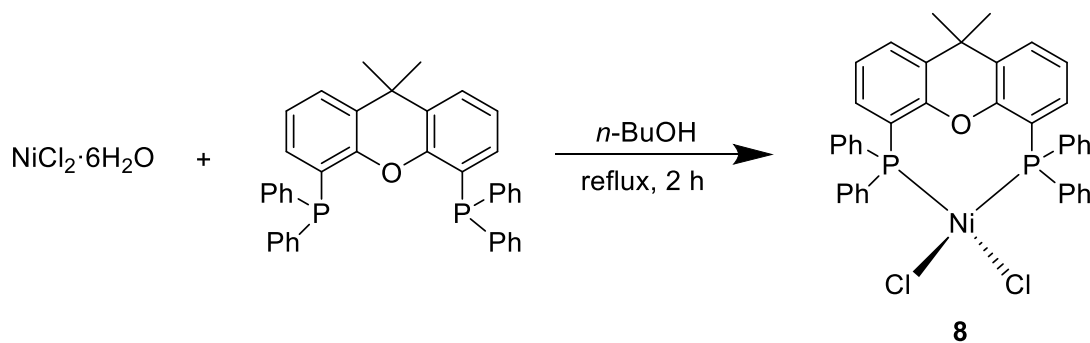


The ^{31}P NMR spectrum of **7a** in benzene- d_6 displays a doublet of doublets centered at 22.4 ppm, which indicates the coupling of two inequivalent P atoms. This is consistent with coordination of the xantphos ligand to a Ni center bearing the unsymmetrically substituted alkyne **1a**. By contrast, the ^{31}P NMR spectrum of **7b** in the same solvent exhibits a singlet at 22.3 ppm, whereas the spectrum of the bis(chelate) complex **6** shows a multiplet at 10.0–8.2 ppm. Relative to free xantphos [$\delta(^{31}\text{P}) = -18.4$ ppm, C_6D_6], the ^{31}P NMR resonance signals of these complexes are all significantly downfield-shifted. In their ^1H NMR spectra, each of the three complexes exhibits a characteristic singlet attributable to the xantphos methyl protons. In case of the alkyne complexes, this singlet is observed at 1.34 and 1.32 ppm for **7a** and **7b**, respectively. For **6**, this singlet is located at 1.44 ppm and thus slightly downfield-shifted from that of free xantphos [$\delta(^1\text{H}) = 1.37$ ppm]. For comparison with **7a** and **7b**, it is noted that the corresponding complexes of the DPEphos ligand were recently reported [DPEphos = (Oxydi-2,1-phenylene)bis(diphenylphosphine)].¹⁸ Those complexes showed analogous ^{31}P NMR signals Wdownfield-shifted by about 6 ppm.

The analytical data for **7a** are consistent with the incorporation of one O atom. This could be a consequence of oxidation of the highly air-sensitive complex. In support, the ESI mass spectrum shows a feature that can be attributed to xantphos oxide. Also found were features that can be assigned to xantphos and an $\{\text{M} - \text{H}\}^+$ ion, which could arise from loss of a hydrogen from the alkyne ligand.

The synthesis of the Ni^{II} complex **8** was based on a method¹⁹ for its preparation as an intermediate that was used without purification and characterization. Thus, the complexation was carried out with equimolar amounts of $\text{NiCl}_2 \cdot 6\text{H}_2\text{O}$ and xantphos in refluxing *n*-butanol, and the crude product precipitated from the reaction mixture at room temperature. After workup and recrystallization, **8** was obtained as a purple crystalline solid in high yield. The composition of **8** was confirmed by elemental analysis and ESI mass spectrometry.

Scheme 14. Synthesis of Complex **8**



3.4 Conclusion

The synthesis and characterization of four xantphos complexes of Ni were described in this Chapter. The bis(chelate) complex **6** was synthesized by a substitution reaction of the Ni⁰ precursor [Ni(cod)₂] with the phosphine ligand. The complex was characterized by ¹H and ³¹P NMR spectroscopy.

The known alkyne complex **7b** was obtained by two methods. First, the literature method was employed with minor modifications. Second, the complex was synthesized by a simpler method that involves sequential addition of an excess of the internal alkyne **1b** and a stoichiometric amount of xantphos to [Ni(cod)₂]. Both methods gave the complex in similar yields. The new alkyne complex **7a** also was synthesized by two methods. In the first method, the terminal alkyne **1a** was substituted for the internal alkyne ligand in **7b**. In the second method, **1a** was substituted for one of the two xantphos ligands in **6**. Because the first method gave the complex in a much higher yield, it is the preferred method. This complex was characterized by ¹H and ³¹P NMR spectroscopy, elemental analysis and mass spectrometry.

The synthesis of the Ni^{II} complex **8** involves the complexation of NiCl₂·6H₂O with xantphos in refluxing *n*-butanol. This complex was characterized by elemental analysis and mass spectrometry.

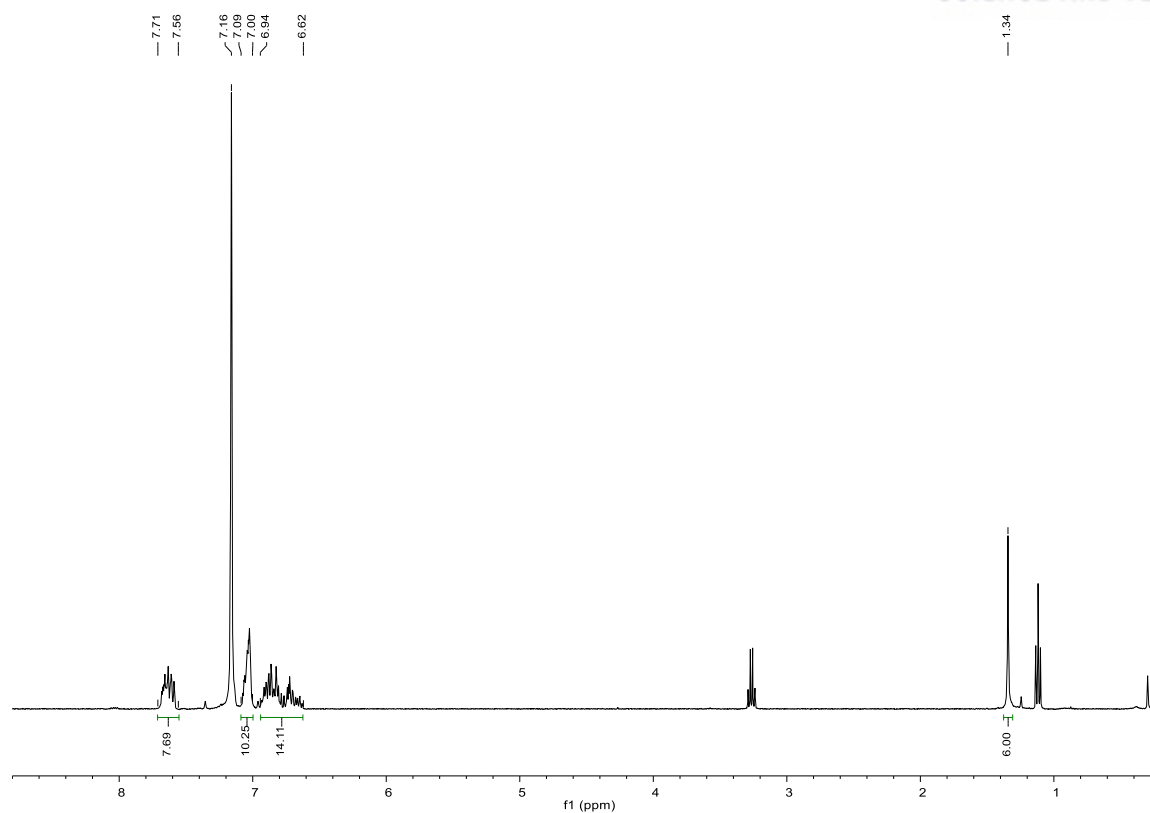


Figure S1. ¹H NMR spectrum of **7a** in benzene-*d*₆ (400 MHz, 25 °C).

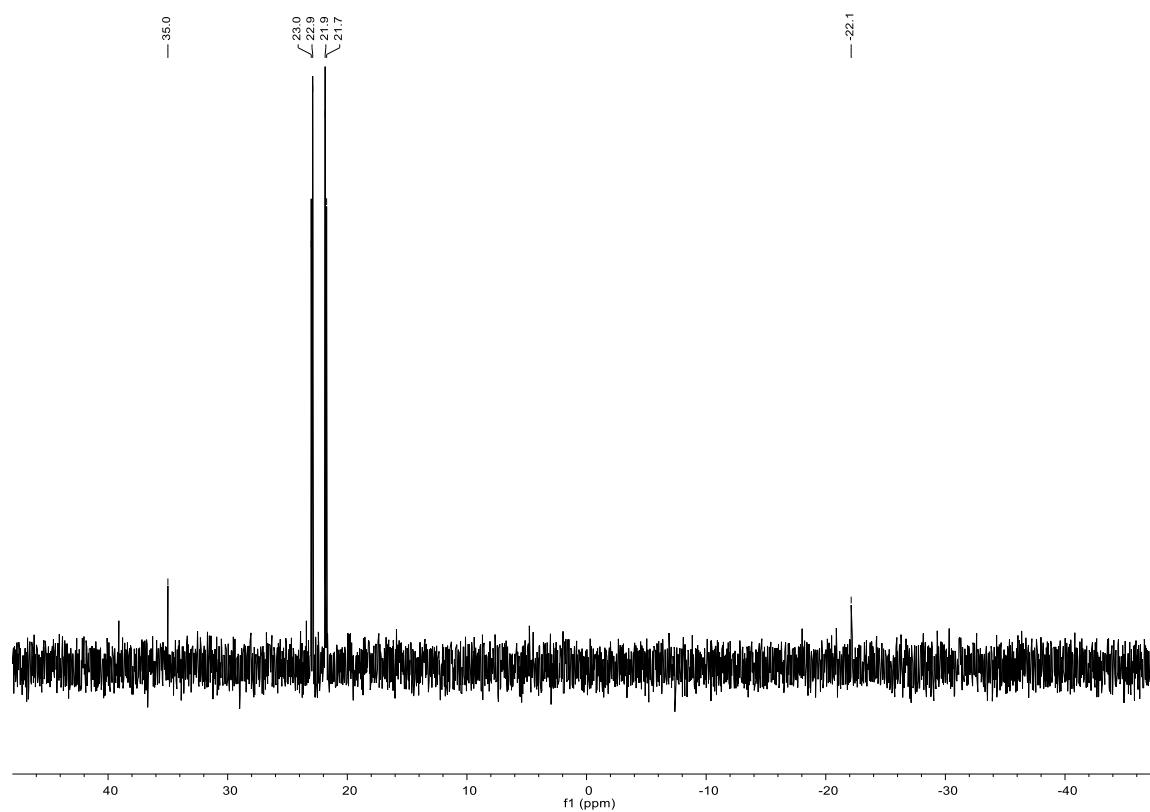


Figure S2. ³¹P NMR spectrum of **7a** in benzene-*d*₆ (162 MHz, 25 °C).

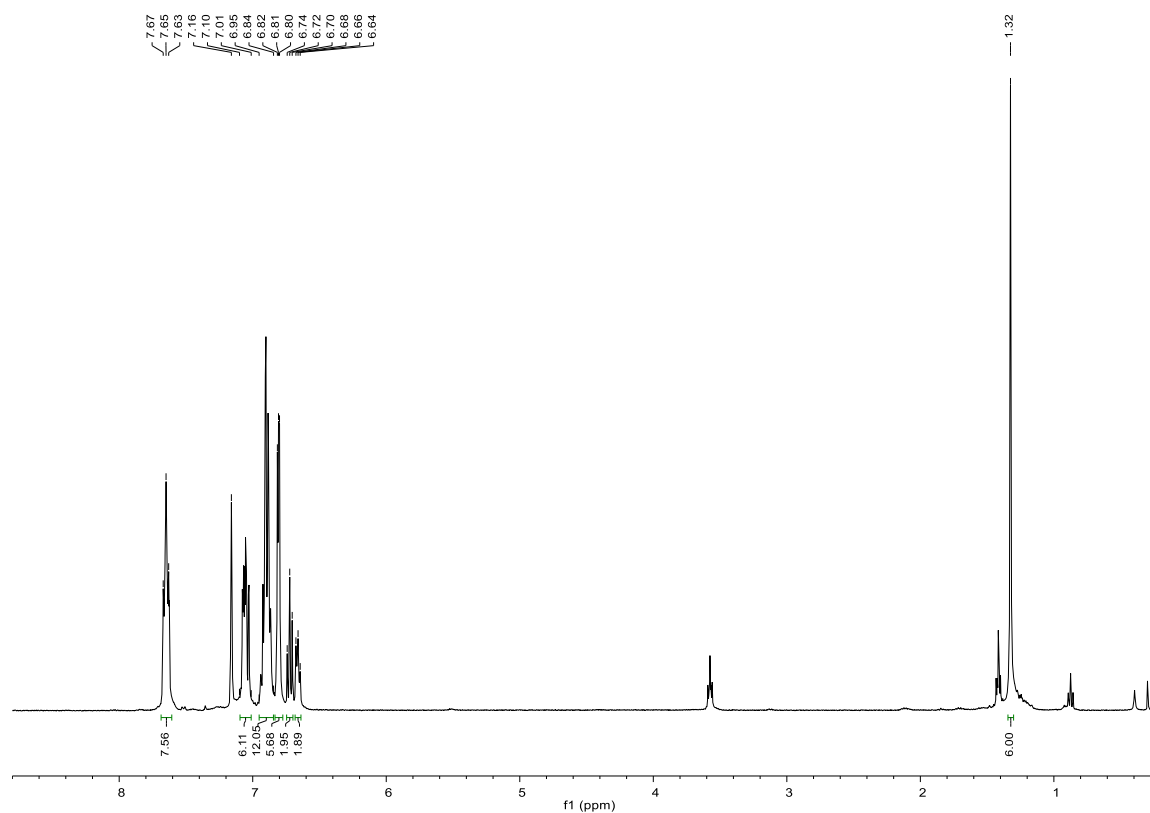


Figure S3. ¹H NMR spectrum of **7b** in benzene-*d*₆ (400 MHz, 25 °C).

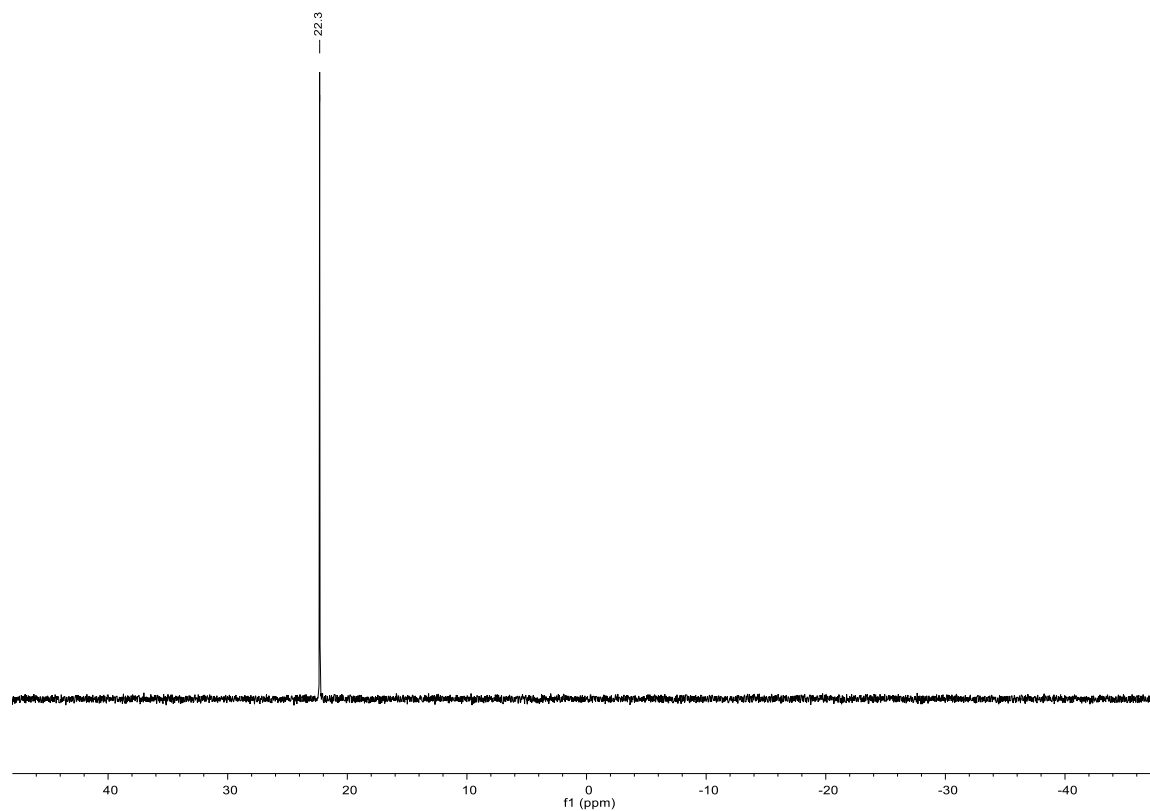


Figure S4. ³¹P NMR spectrum of **7b** in benzene-*d*₆ (162 MHz, 25 °C).

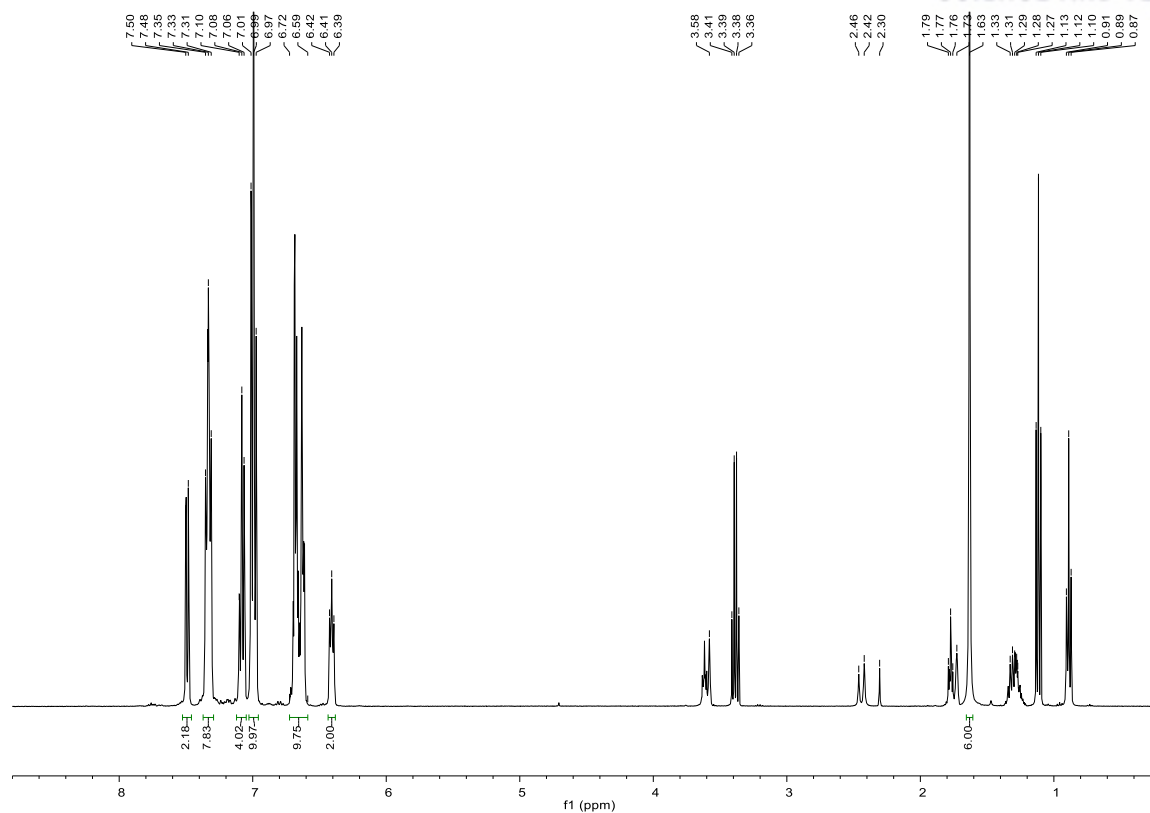


Figure S5. ¹H NMR spectrum of **7b** in tetrahydrofuran-*d*₈ (400 MHz, 25 °C).

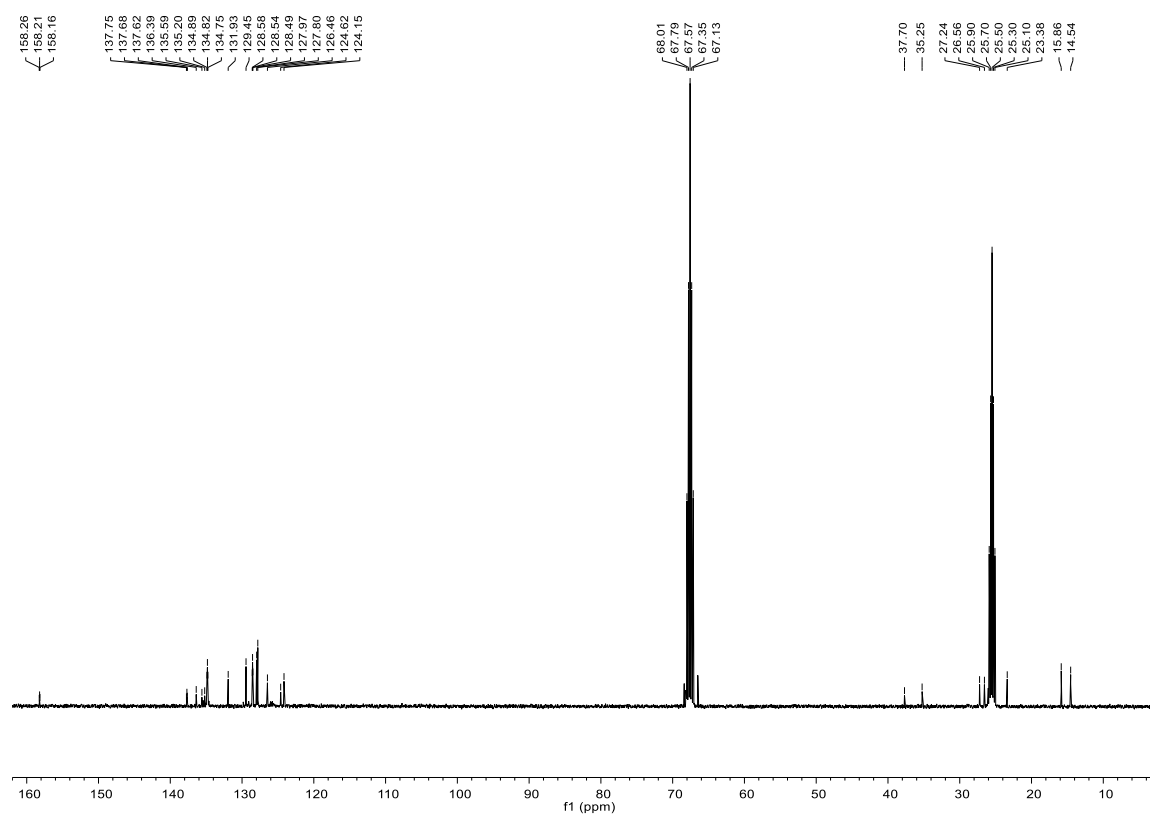


Figure S6. ¹³C NMR spectrum of **7b** in tetrahydrofuran-*d*₈ (101 MHz, 25 °C).

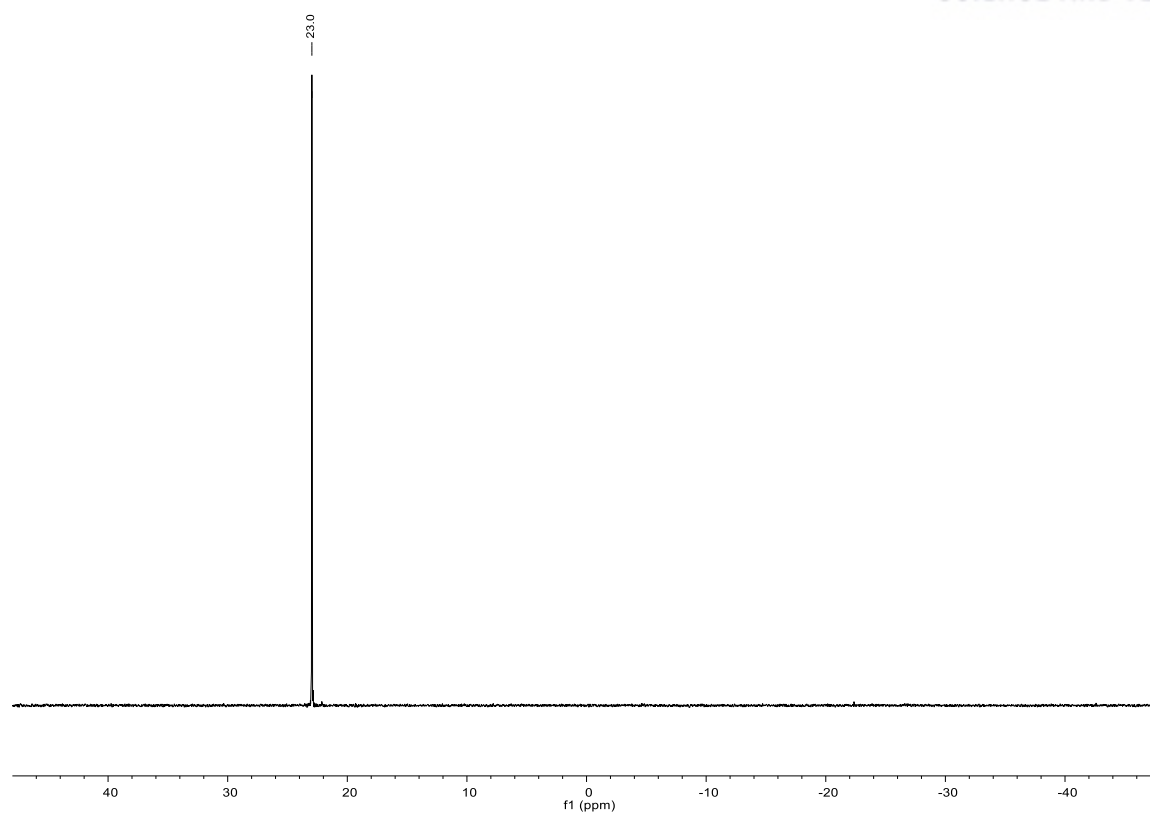


Figure S7. ^{31}P NMR spectrum of **7b** in tetrahydrofuran- d_8 (162 MHz, 25 °C).

Chapter 4

Investigation of the Azide–Alkyne Cycloaddition with Nickel Complexes

4.1 Introduction

The investigation of the azide–alkyne cycloaddition will be the focus of Chapter 4. The catalytic activity of the complexes described in Chapter 3 was explored in reactions of benzylazide (**2**) with the terminal alkyne **1a** and the internal alkyne **1b** in toluene. Because of the air-sensitivity of the Ni⁰ complexes, the reactions were investigated under inert atmosphere. The activity of **6** was also examined in air with either toluene or H₂O as solvent.

To gain insights into the mechanism of the NiAAC, catalytic and stoichiometric reactions of **6** and **7a** were studied by NMR spectroscopy. Furthermore, the reaction of the original [NiCp₂]/xantphos system was revisited by NMR spectroscopy. Finally, reactions of [NiCp₂] with xantphos were investigated to probe the formation of xantphos complexes of Ni⁰.

4.2 Experimental Section

4.2.1 Materials and Methods

Materials. All reagents and solvents were purchased from commercial sources and were used as received, unless noted otherwise. Toluene was deoxygenated by sparging with N₂ and purified by passage through two packed columns of molecular sieves under an N₂ pressure (MBraun solvent purification system). [NiCp₂] was purchased from Sigma-Aldrich, xantphos, >98.0 %, from Tokyo Chemical Industry Co., and xanthene, 98%, from Acros. Benzylazide (**2**) was synthesized by a previously reported method.^{13,20} Preparation and handling of air- and moisture-sensitive materials were carried out under an inert gas atmosphere by using either standard Schlenk and vacuum line techniques or a glovebox.

Physical Methods. NMR spectra were recorded on a Bruker Avance III 400 spectrometer at ambient temperature. ¹H, ¹³C and ³¹P chemical shifts are reported in parts per million (ppm) and were referenced to residual solvent peaks (for ¹H and ¹³C NMR spectra) or an external standard [triphenyl phosphate (0.0485 M in acetone-*d*₆, −17.57 ppm) for ³¹P NMR spectra].

4.2.2 Procedure for the Nickel-Catalyzed Azide–Alkyne Cycloaddition

To determine the catalytic activity of the Ni complexes synthesized in this work, the procedure¹³ for the azide–alkyne cycloaddition catalyzed by [NiCp₂]/xantphos was used with modifications. In an N₂ atmosphere, a mixture of 0.038 mmol (10 mol %) of Ni complex in 2.0 ml of toluene was treated with 50 μl (48 mg, 0.46 mmol) of **1a** or 84 mg (0.46 mmol) of **1b** (98 %; 1.2 equiv with respect to **2**) and 48 μl (51 mg, 0.38 mmol) of **2**. The reaction mixture was stirred at room temperature for 90 min. The subsequent work-up was carried out in air. The mixture was diluted with dichloromethane and the organic phase washed with H₂O and dried over Na₂SO₄. The 1,2,3-triazole products were separated and purified by flash column chromatography on silica gel. The yields of the 1,2,3-triazoles are given in Table 1 in Section 4.3.1. Reactions of **6** in air were performed in the same manner with either toluene or H₂O as the solvent and either in the absence or in the presence of 124 mg (0.38 mmol) of Cs₂CO₃ as additive (Table 2).

4.2.3 Preparation of Reaction Solutions for NMR Spectroscopy

Solutions were prepared in an N₂ atmosphere and xanthene was added as a standard, as described below. The reaction solutions were briefly and vigorously shaken and the progress of the reactions was monitored by ¹H NMR spectroscopy. The concentrations of the reactants and products were estimated by comparing the integration of the xanthene methylene proton signal (δ, 3.56 ppm, 2 H) with the integrations of the xantphos methyl proton signal (δ, 1.37 ppm, 6 H), the methyl proton signal of **6** (δ, 1.44 ppm, 12 H), the methyl proton signal of **7a** (δ, 1.34 ppm, 6 H), the alkyne proton

signal of **1a** (δ , 2.71 ppm, 1 H), the benzyl proton signal of **2** (δ , 3.67 ppm, 2 H), the benzyl proton signal of **3a** (δ , 5.03 ppm, 2 H), and the benzyl proton signal of **4** (δ , 4.83 ppm, 2 H). In addition, ^{31}P NMR spectra were recorded at the end of the reactions. Time courses of the reactions and ^1H and ^{31}P NMR spectra of the product solutions are shown in Section 4.3.2.

Catalytic Reactions of 6 and 7a. A solution of 0.6 mg (0.5 μmol , 1 mol %) of **6** and 9.3 mg (50 μmol) of xanthene (98 %) in 0.40 ml of C_6D_6 was placed in an NMR tube. A stock solution of 3.7 mg (5.0 μmol) of **7a** in 0.10 ml of C_6D_6 was prepared. A solution of 0.50 μmol (0.010 ml of the 50 mM stock solution, 1 mol %) of **7a** and 9.3 mg (50 μmol) of xanthene in 0.40 ml of C_6D_6 was placed in an NMR tube. To each complex solution was added a solution of 6.7 μl (6.3 mg, 60 μmol) of **1a** and 6.3 μl (6.7 mg, 50 μmol) of **2** in 0.10 ml of C_6D_6 .

Reactions of 6 and 7a with Individual Substrates. The following stock solutions were prepared: 16.8 μl (15.6 mg, 150 μmol) of **1a** in 0.30 ml of C_6D_6 , 19.0 μl (20.2 mg, 150 μmol) of **2** in 0.30 ml of C_6D_6 , 3.7 mg (5.0 μmol) of **7a** in 0.10 ml of C_6D_6 , and 9.3 mg (50 μmol) of xanthene in 0.10 ml of C_6D_6 . **Reactions of 6 with 1a or 2.** Two solutions of 0.6 mg (0.5 μmol) of **6** and 5.0 μmol (0.010 ml of the 500 mM stock solution) of xanthene in 0.40 ml of C_6D_6 were placed in separate NMR tubes. To one of these solutions was added a solution of 5.0 μmol (0.010 ml of the 500 mM stock solution) of **1a** in 0.10 ml of C_6D_6 . To the other solution was added a solution of 5.0 μmol (0.010 ml of the 500 mM stock solution) of **2** in 0.10 ml of C_6D_6 . **Reaction of 7a with 2.** A solution of 0.5 μmol (0.010 ml of the 50 mM stock solution) of **7a** and 5.0 μmol (0.010 ml of the 500 mM stock solution) of xanthene in 0.40 ml of C_6D_6 was placed in an NMR tube. To this solution was added a solution of 5.0 μmol (0.010 ml of the 500 mM stock solution) of **2** in 0.10 ml of C_6D_6 .

Catalytic Reaction of [NiCp₂]/Xantphos. A solution of 5.8 mg (10 μmol , 10 mol %) of xantphos, 13.4 μl (12.5 mg, 120 μmol) of **1a**, 12.7 μl (13.3 mg, 100 μmol) of **2**, and 18.6 mg (100 μmol) of xanthene in 0.30 ml of C_6D_6 was placed in an NMR tube. A solution of 1.9 mg (10 μmol , 10 mol %) of [NiCp₂] in 0.20 ml of C_6D_6 was added.

Reactions of [NiCp₂]. Reactions of [NiCp₂] with Xantphos. A solution of 0.9 mg (5 μmol) of [NiCp₂], 28.9 mg (50 μmol) of xantphos and 9.3 mg (50 μmol) of xanthene in 0.50 ml of C_6D_6 was prepared and monitored by NMR spectroscopy. **Reactions of [NiCp₂] with Xantphos, 1a and 2.** A solution of 0.9 mg (5 μmol) of [NiCp₂], 9.3 mg (15 μmol) of xantphos and 9.3 mg (50 μmol) of xanthene in 0.47 ml of C_6D_6 was prepared. To this solution were added 0.020 ml (10 μmol) of the 500 mM stock solution of **1a** in C_6D_6 and 0.010 ml (5 μmol) of the 500 mM stock solution of **2** in C_6D_6 . The reaction solution was then transferred into an NMR tube.

4.3 Results and Discussion

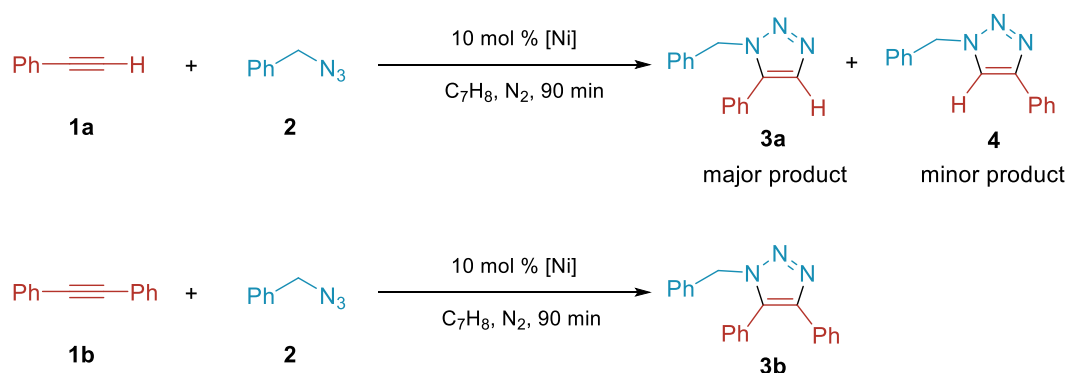
4.3.1 Catalytic Studies

The catalytic activity of the complexes described in Chapter 3 was explored in reactions of **2** with the terminal alkyne **1a** and the internal alkyne **1b** in toluene. Because of the air-sensitivity of the Ni⁰ complexes, the reactions were performed under an N₂ atmosphere. Otherwise, the standard conditions for the NiAAC were employed.¹³ The work described in this section was performed in collaboration with Dr. Woo Gyum Kim and Prof. Sung You Hong, who provided azide **2** and carried out the separation of the 1,2,3-triazole products. Complex **5** was synthesized by Jungha Lee according to a procedure to be reported elsewhere.¹⁵ Also some of the reaction solutions for the experiments shown in Table 1 were prepared by Jungha Lee.

At the outset of this study, the excellent yield reported for the reaction of **2** with the terminal alkyne **1a** catalyzed by [NiCp₂]/xantphos/Cs₂CO₃ (1:1:10) in air (91 % for **3a** and 6 % for **4**) was reproduced here under N₂ (Table 1, entry 1). Next, the effect of Cs₂CO₃ was investigated. While this additive significantly improved the yield of **3a** for the reaction in air,¹³ it was found to have only a marginal effect on the reaction under N₂ (entry 2).

Having established these points of reference, attention was turned to the Ni(xantphos) complexes. Complexes **5**, **6** and **7a** produced isolated yields of over 85 % of **3a** and ≤6 % of **4** (entries 3–5), similar to yields obtained with the [NiCp₂]/xantphos system. Interestingly, also an equimolar mixture of the Ni⁰ precursor [Ni(cod)₂] and the phosphine ligand gave a high yield of **3a** (entry 7). In contrast, [Ni(cod)₂] used without xantphos gave only a trace amount of **3a** (entry 8). The Ni^{II} complex **8** was ineffective (entry 9). It is noteworthy that complexes **5**, **6** and **7a** each yielded a ratio of regioisomers (**3a** and **4**) similar to that found for the [NiCp₂]/xantphos mixture, suggesting that they may share the same active catalyst.

Subsequently, the reaction of **2** with the internal alkyne **1b** was investigated. Surprisingly, the [NiCp₂]/xantphos /Cs₂CO₃ combination, which is highly active in catalyzing the formation of **3b** in air, failed when used under N₂ (entries 1 and 2). Nevertheless, **5**, **6** and **7b** afforded **3b** in excellent yields of over 90 %. Even the combination of [Ni(cod)₂] and xantphos showed an only slightly lower activity, as it did for the formation of **3a**. As expected, **8** was ineffective, while [Ni(cod)₂] gave **3b** in a poor yield.

Table 1. Catalytic Activity of Ni Complexes in the Alkyne–Azide Cycloaddition^a


Entry	Catalyst	Reaction with 1a		Reaction with 1b
		Yield (%) ^b		Yield (%) ^b
		3a	4	3b
1	NiCp ₂ /xantphos/Cs ₂ CO ₃ (1:1:10) ^c	90	5	4
2	NiCp ₂ /xantphos (1:1)	86	5	<2
3	NiCp(xantphos) (5)	92	6	92
4	Ni(xantphos) ₂ (6)	93	6	94
5	Ni(xantphos)(PhCCH) (7a)	87	6	
6	Ni(xantphos)(PhCCPh) (7b)			97
7	Ni(cod) ₂ /xantphos (1:1)	87	6	87
8	Ni(cod) ₂	trace		17
9	Ni(xantphos)Cl ₂ (8)	–	–	trace

^aReaction conditions: 0.46 mmol of **1a** or **1b** (1.2 equiv with respect to **2**), 0.38 mmol of **2** and 0.038 mmol (10 mol %) of catalyst in 2.0 ml of toluene, N₂ atmosphere; reaction time, 90 min.

^bIsolated yield; average of two experiments; dash = product not detected by thin-layer chromatography (TLC); trace = product detected by TLC but not isolated. ^c0.38 mmol of Cs₂CO₃ (1.0 equiv with respect to **2**).

Because **6** is moderately air-stable in the solid state, its activity in air was investigated as well. In this context, it is relevant to note that the reaction mixture is a suspension because of the low solubility of this complex. For comparison, results from the reaction of **1a** with **2** catalyzed by [NiCp₂]/xantphos, both with and without the additive Cs₂CO₃, are shown in Table 2 (entries 1–3). Although **6** failed in the absence of Cs₂CO₃ (entry 4), its catalytic activity was preserved in air with either toluene or H₂O as solvent when the additive was present (entries 5 and 6). Thus, **6** matches the catalytic activity of [NiCp₂]/xantphos.

The role of the additive is currently not understood and requires further study. The results from reactions conducted under N₂ demonstrate that it is not required for the cycloaddition of the two substrates.

Table 2. Catalytic Activity of [NiCp₂]/Xantphos and **6** in the Alkyne–Azide Cycloaddition in Air^a

Entry	Catalyst	Additive ^b	Solvent	Reaction with 1a	
				Yield (%) ^c	
				3a	4
1	NiCp ₂ /xantphos (1:1)		toluene	58	6.9
2	NiCp ₂ /xantphos (1:1)	Cs ₂ CO ₃	toluene	91 ^d	6 ^d
3	NiCp ₂ /xantphos (1:1)	Cs ₂ CO ₃	H ₂ O	91 ^d	6 ^d
4	Ni(xantphos) ₂ (6)		toluene	5	–
5	Ni(xantphos) ₂ (6)	Cs ₂ CO ₃	toluene	90	6.5
6	Ni(xantphos) ₂ (6)	Cs ₂ CO ₃	H ₂ O	91	7.5

^aReaction conditions: 0.46 mmol of **1a** (1.2 equiv with respect to **2**), 0.38 mmol of **2** and 0.038 mmol (10 mol %) of catalyst in 2.0 ml of toluene or H₂O, in air; reaction time, 90 min. ^bIsolated yield; average of two experiments; dash = product not detected by thin-layer chromatography (TLC). ^cFrom ref 13. ^d0.38 mmol of Cs₂CO₃ (1.0 equiv with respect to **2**).

4.3.2 NMR Spectroscopic Studies

To gain insights into the nature of the catalytically active species and the mechanism by which the NiAAC operates, an NMR spectroscopic study of reactions involving complexes **6** and **7a** and the [NiCp₂]/xantphos system was undertaken. To eliminate any effect of O₂ on the reactions and to ensure the stability of the Ni⁰(xantphos) catalysts, the reactions were performed under N₂.

Catalytic Reactions of 6a and 7. In the course of this study, complexes **6** and **7a** were found to exhibit high catalytic activity in the reaction of **2** with **1a** even with a lower catalyst loading of only 1 mol %. Time courses reflecting the concentration changes of the compounds in solution relative to xanthene added as a standard were obtained by ¹H NMR spectroscopy (see the Experimental Section for details). These time courses are shown in Figures 1 and 2 and indicate clean conversion of the substrates into the 1,2,3-triazoles, which were formed in yields of 95 and 5 % for **3a** and **4**, respectively, in both cases. As expected, about 0.2 equiv of **1a**, which was added in excess, remained. Complex **7a** is somewhat more efficient than **6**, as the conversion was completed in about 20 min, compared with about 50 min for **6**.

The ¹H NMR spectra of the product solutions, shown in Figures S8 and S9, exhibit the resonance signals of the benzyl protons in **3a** (5.03 ppm), the benzyl protons in **4** (4.83 ppm), the methylene protons of the internal standard (xanthene, 3.56 ppm) and the alkyne proton of remaining **1a** (2.71 ppm).

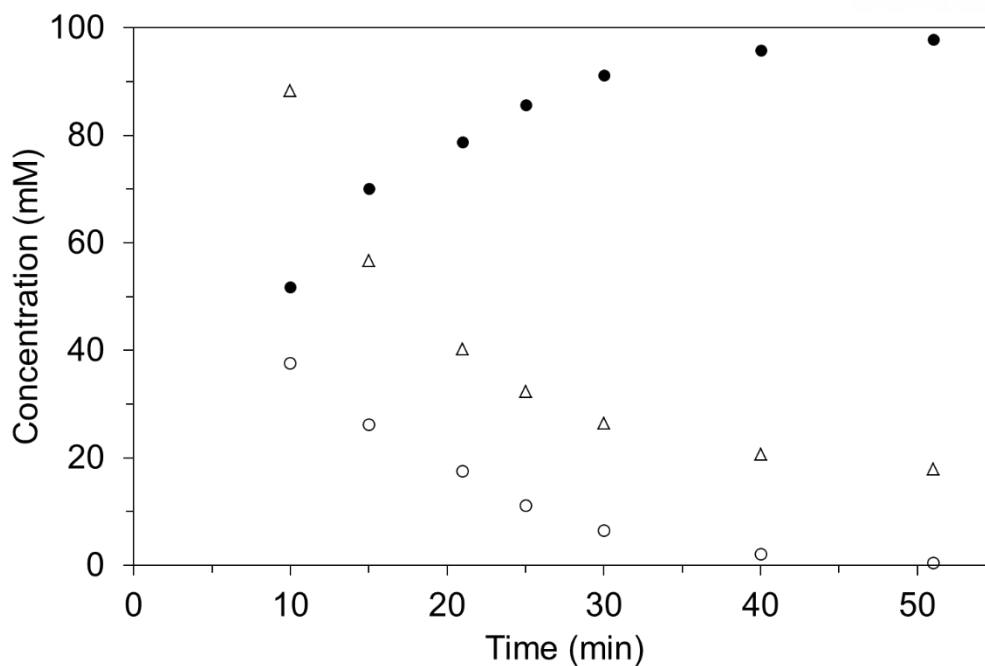


Figure 1. Time course (^1H NMR, 400 MHz, 25 $^\circ\text{C}$) of the reaction of 100 mM **2** (open circles) with 1.2 equiv of **1a** (open triangles) in the presence of 1 mM (1 mol %) **6** in benzene- d_6 , producing **3a** (solid circles).

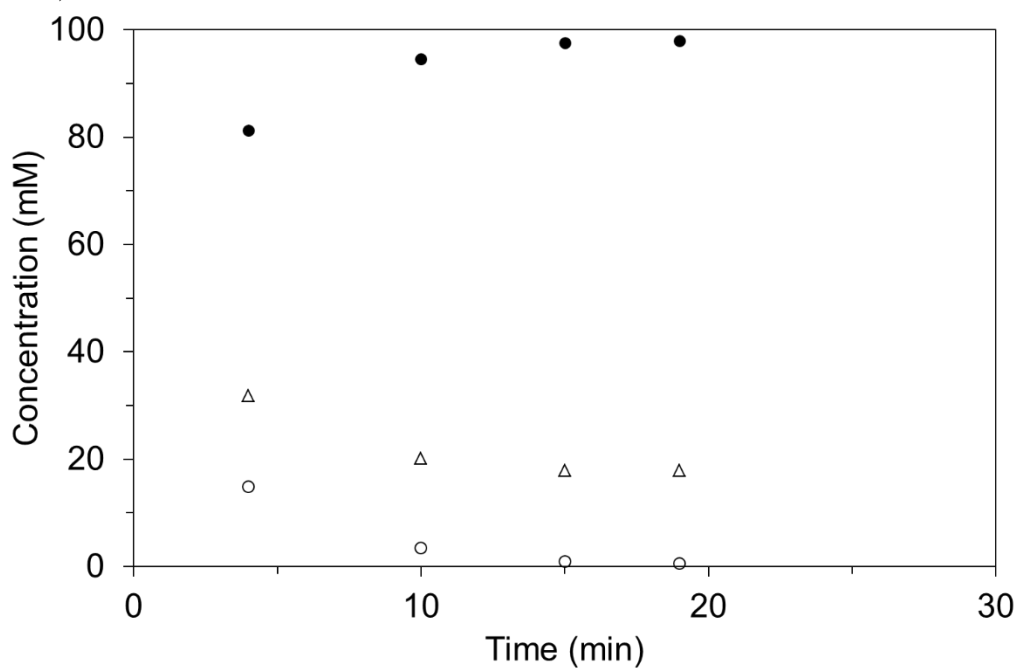
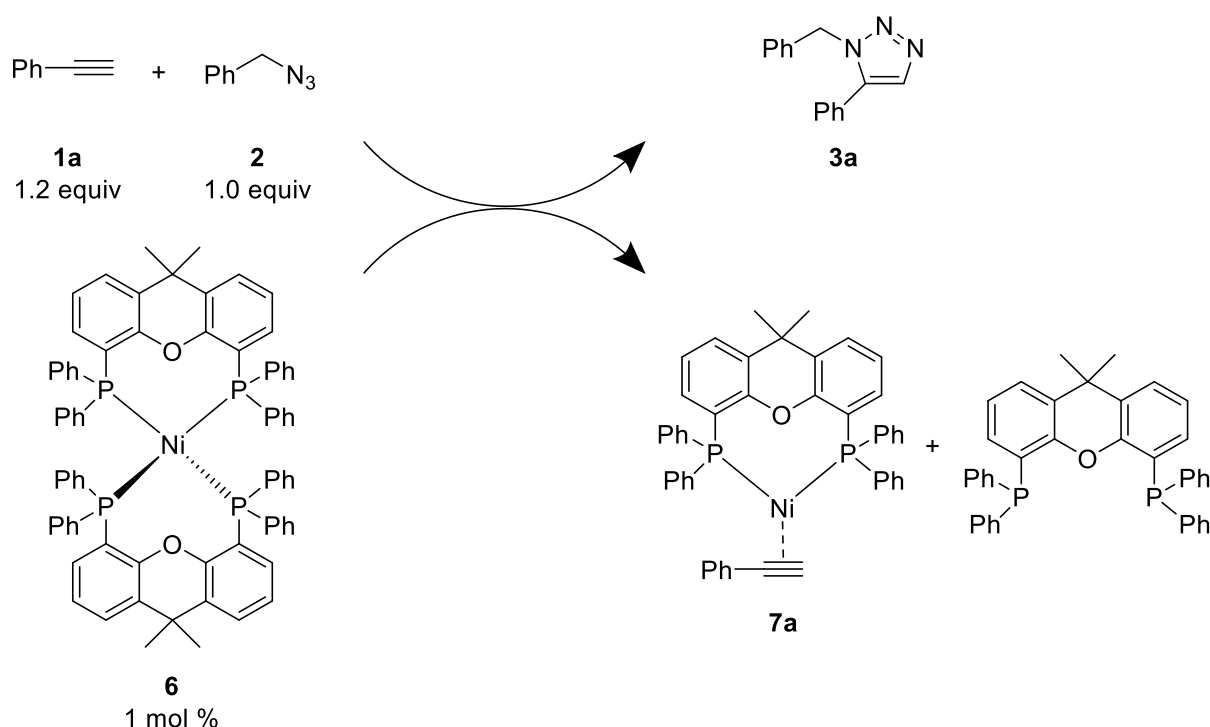


Figure 2. Time course (^1H NMR, 400 MHz, 25 $^\circ\text{C}$) of the reaction of 100 mM **2** (open circles) with 1.2 equiv of **1a** (open triangles) in the presence of 1 mM (1 mol %) **7a** in benzene- d_6 , producing **3a** (solid circles).

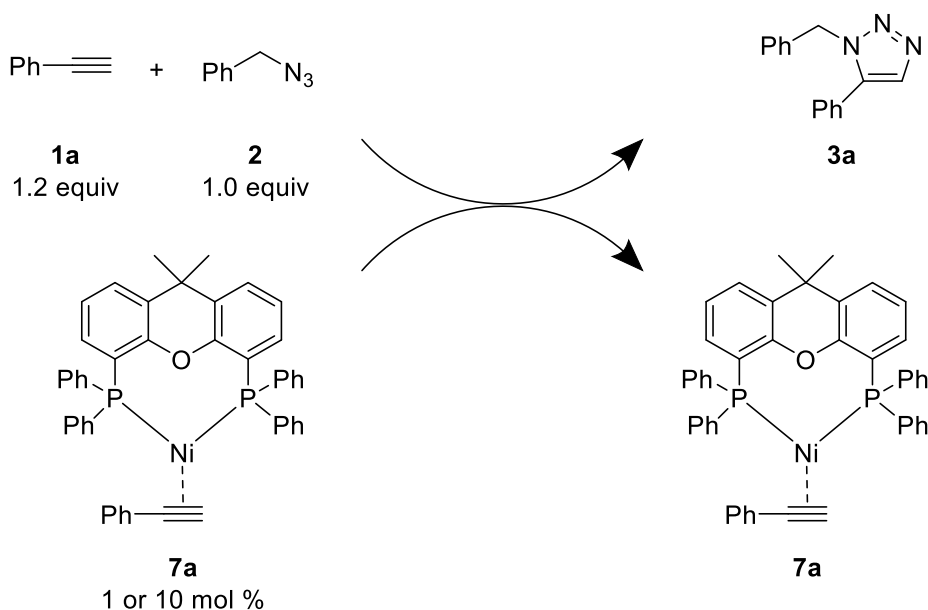
Notably, the spectra also offer insights into the fate of the Ni complexes. For the reaction catalyzed by **6**, the characteristic singlets of **7a** and free xantphos were observed at 1.35 and 1.37 ppm, respectively, whereas the singlet of **6** at 1.44 ppm was substantially diminished. The integrations of these resonance signals account for 0.5 equiv of **7a**, 0.6 equiv of xantphos and <0.05 equiv of **6** (with respect to the initial concentration of **6**). The presence of **7a** and free xantphos is also supported by the characteristic resonance signals observed in the ^{31}P NMR spectrum of the product solution, albeit they are of very low intensity because of the low catalyst loading in this experiment. Taken together, these results indicate that **6** is converted into **7a** and free xantphos during catalysis (Scheme 15).

Scheme 15. Reaction of **6** with **1a** and **2**



For the reaction catalyzed by **7a**, the catalyst remained largely intact throughout the reaction, with about 0.7 equiv found in the product solution. About 0.2 equiv of uncoordinated xantphos accounts for some decomposition of the catalyst. To obtain data for **7a** of higher quality, the reaction was also performed at a higher catalyst loading of 10 mol %. (The solubility of **7a** is substantially greater than that of **6**, whose solubility limit is about 2 mM.) Under these conditions, the reaction was completed within 4 min to yield 95 % of **3a** and 5 % of **4**. Moreover, 83 % of **7a** was still present. Its identity was confirmed by a doublet of doublets at 22.4 ppm in its ^{31}P NMR spectrum (Figure S10). This spectrum also showed signals at -22.1, 23.5 and 25.1 ppm, which may be due to decomposition of the catalyst. This reaction is summarized in Scheme 16.

Scheme 16. Reaction of **7a** with **1a** and **2**



Reactions of **6 and **7a** with Individual Substrates.** To develop an understanding of possible steps of the catalytic mechanism, the reactions of **6** and **7a** with individual substrates were investigated. When 10 equiv of **1a** were added to a 1 mM solution of **6**, the conversion into **7a** and xantphos took less than 2 h. The time course for product formation is shown in Figure 3 and the ^1H and ^{31}P NMR spectra are shown in Figure S11. Under the same conditions, **6** reacted much more slowly with **2**, releasing only about 0.5 equiv of xantphos over the same time frame (Figure 3). Although new resonance signals were detected in the ^1H and ^{31}P NMR spectra, the identity of the Ni product was not clarified at this time.

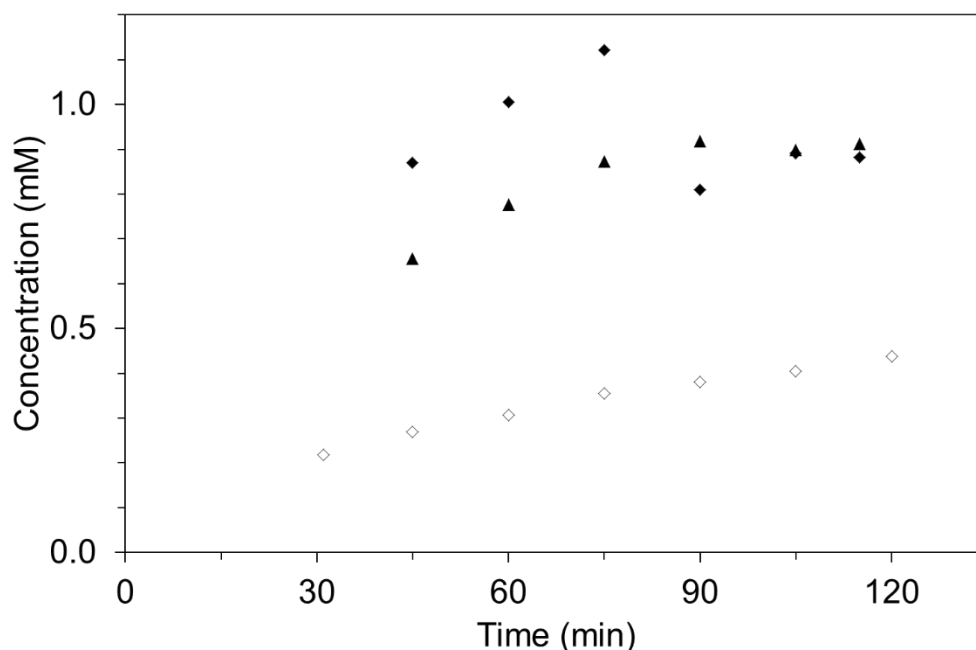
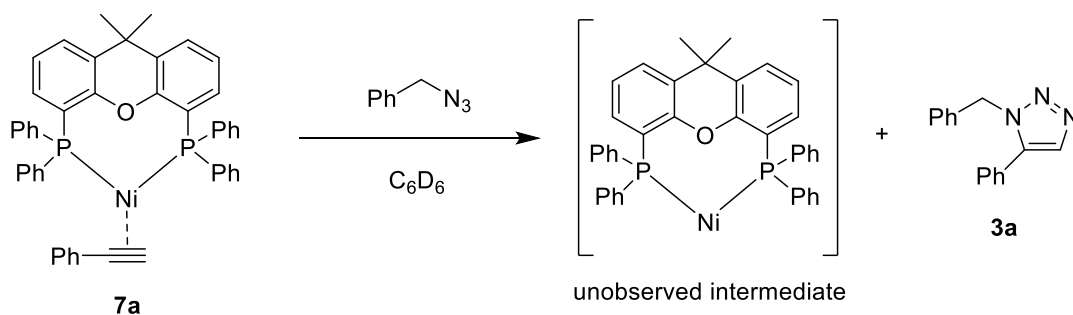


Figure 3. Time courses (^1H NMR, 400 MHz, 25 °C) of the reactions of 1 mM **6** with a) 10 equiv of **1a** and b) 10 equiv of **2** in benzene- d_6 , showing the formation of **7a** [a) solid triangles] and the release of xantphos [a) solid diamonds and b) open diamonds].

Alkyne complex **7a** reacted rapidly with 10 equiv of **2** to form the corresponding 1,2,3-triazole within 4 min. Solutions of 1 mM and 10 mM **7a** gave **3a** in yields of 75 and 65 %, respectively, and <4 % of **4** (Figure S12). As shown in Scheme 17, the initial Ni product of this reaction presumably is the 14-electron $\text{Ni}^0(\text{xantphos})$ fragment, which may be expected to be highly reactive and undergo further reaction with **2**. Indeed, the ^{31}P NMR spectra of the product solutions of this reaction and of the reaction of **6** with **2** each show resonance signals at 23.4 and -22.1 ppm, which may be related to common xantphos products of these reactions.

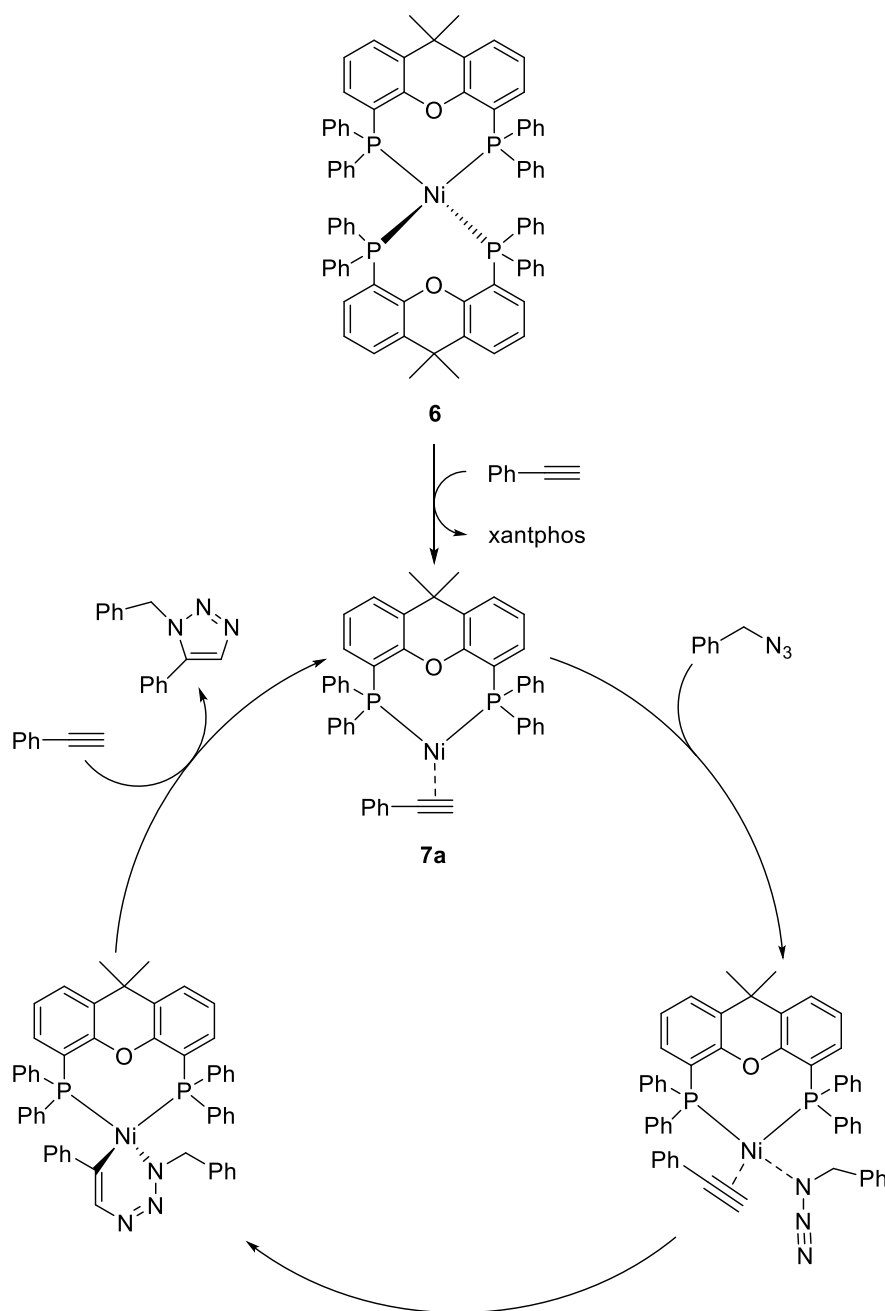
Scheme 17. Production of Triazole **3a** from Reaction of **7a** with **2**



This study provides useful information for the mechanism of the AAC catalyzed by **6** (Scheme 18). When both substrates are present, **6** may react more rapidly with **1a** to afford the alkyne complex **7a**

with concomitant release of xantphos. In turn, **7a** may quickly react with **2** to produce the 1,2,3-triazole giving Ni(xantphos) in the process. If the latter is intercepted by **1a**, the alkyne complex **7a** can be regenerated, thereby closing the catalytic cycle. On the other hand, reaction of Ni(xantphos) with **2** may lead to decomposition of the azide. In principle, Ni(xantphos) may also react with free xantphos present to give **6**. But this may then be converted into the catalytically active **7a**. This mechanism is consistent with the observations made in the stoichiometric and catalytic NMR experiments.

Scheme 18. Proposed Mechanism for the NiAAC Using **6**



Catalytic Reaction of [NiCp₂]/Xantphos. With the stoichiometric and catalytic reactivity of the Ni⁰(xantphos) complexes established, the original [NiCp₂]/xantphos catalyst system was scrutinized. When the reaction of **1a** with **2** in the presence of 10 mol % of [NiCp₂]/xantphos was carried out on a scale suitable for monitoring by NMR spectroscopy (0.010 mmol of **2** in 0.5 ml of C₆D₆ vs. 0.38 mmol of **2** in 2 ml of C₇H₈), it was substantially slower than the reaction described in Section 4.3.1 (6 h vs. <90min). Apparently, not only the concentrations but also the amounts of the reactants affect the reaction. The yields of **3a** and **4** were 87 and 5 %, respectively, The time course for the conversion of the substrates into 1,2,3-triazole, shown in Figure 4, reveals an induction period, which persists for about 1 h. This suggests that a slow catalyst formation step precedes the catalytic reaction. Furthermore, the concentration of free xantphos decreased throughout the reaction and, in particular, at early stages. Based on the results for the reactions catalyzed by **6** and **7a**, free xantphos is not required for 1,2,3-triazole formation. Presumably xantphos is consumed in the catalyst formation step.

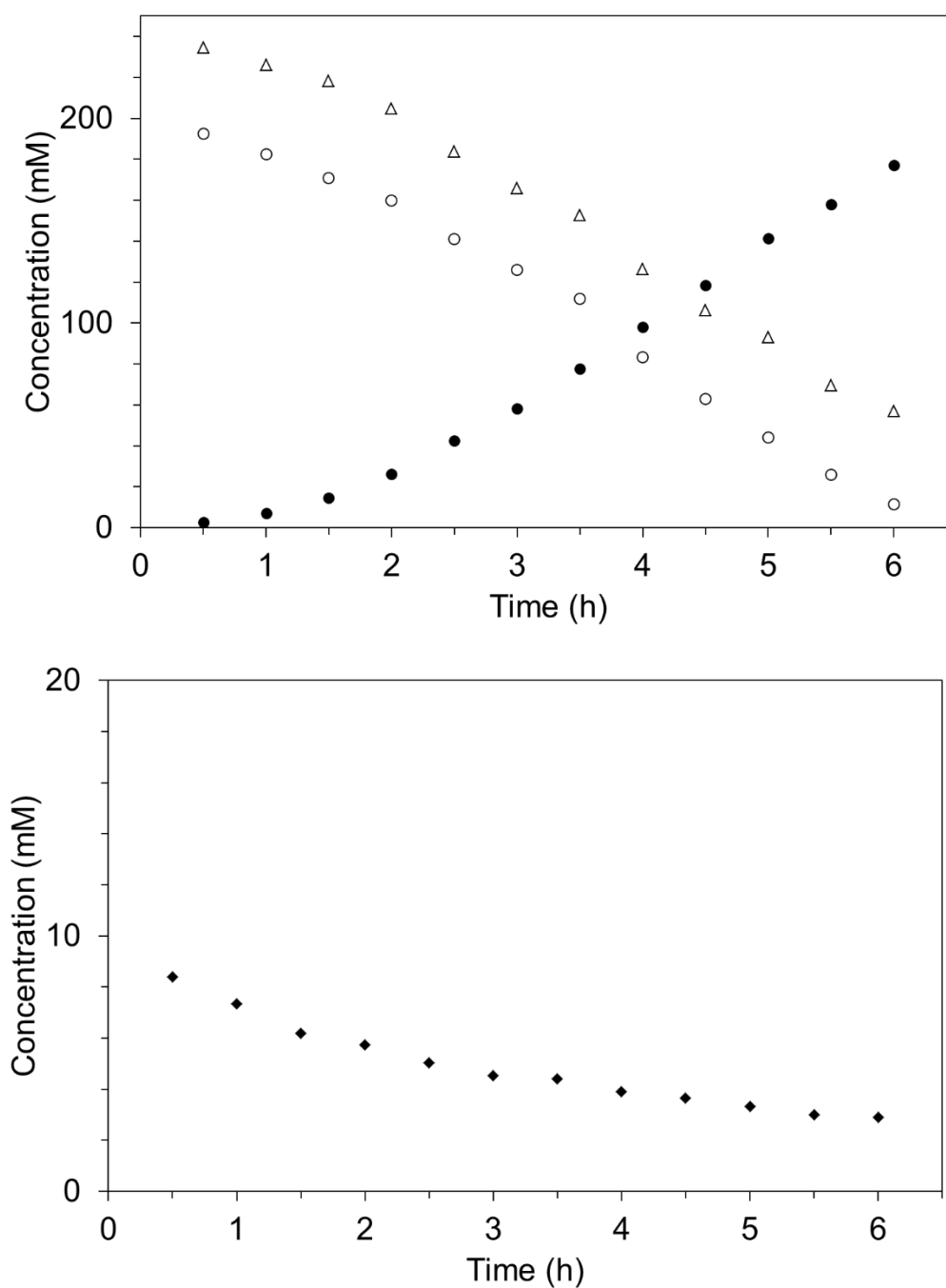


Figure 4. Time course (^1H NMR, 400 MHz, 25 $^\circ\text{C}$) of the reaction of 200 mM **2** with 1.2 equiv of **1a** in the presence of 20 mM (10 mol %) NiCp_2 and xantphos in benzene- d_6 . Top: Conversion of **1a** (open triangles) and **2** (open circles) into **3a** (solid circles). Bottom: xantphos (solid diamonds).

Reactions of [NiCp₂]. In the literature, reactions of [NiCp₂] with mono- and bidentate phosphine ligands have been reported to give NiCp(P-ligand)₂ and Ni(P-ligand)₄ complexes.²¹⁻²⁴ Those reactions were typically performed at elevated temperatures. In the reaction of [NiCp₂] with xantphos, which was studied at room temperature, **5** and **6** were detected by EPR spectroscopy and mass spectrometry, respectively.¹³ Here, the reaction was studied by NMR spectroscopy to obtain more comprehensive evidence for the formation of **6**. Because the reaction was found to be slow, an excess of 10 equiv of xantphos was used. After 48 h, about 16 % of the [NiCp₂] was converted into **6** (Figure 5), which was identified by a singlet at 1.44 ppm in its ¹H NMR spectrum and a multiplet at 10.0–8.2 ppm in its ³¹P NMR spectrum (Figure S14).

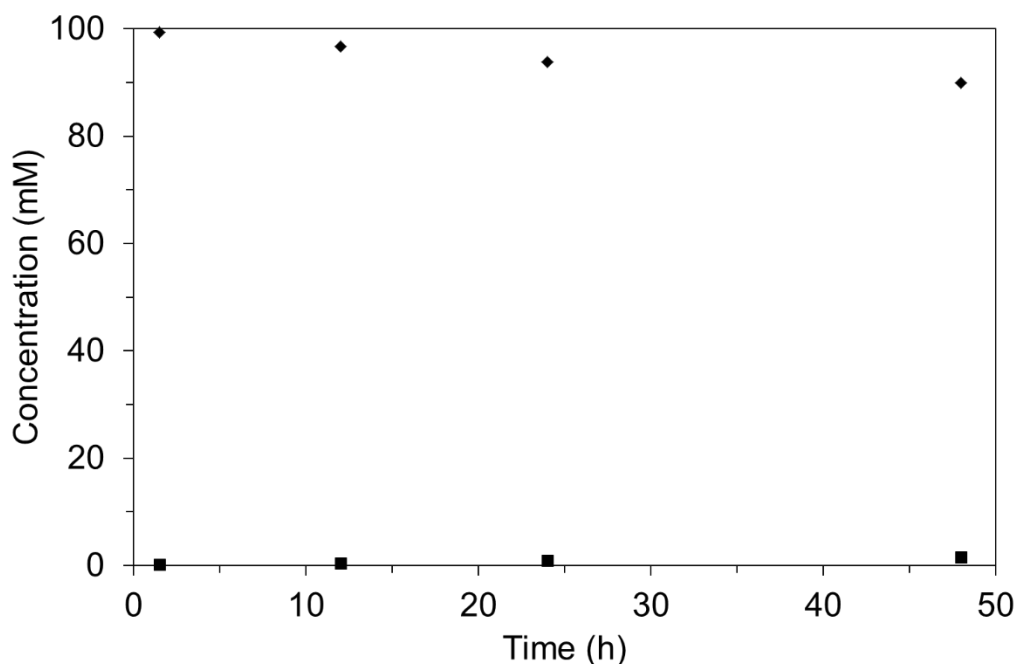


Figure 5. Time course (¹H NMR, 400 MHz, 25 °C) of the reaction of 10 mM NiCp₂ with 10 equiv of xantphos in benzene-*d*₆, showing the formation of **6** (solid squares) and the change in the concentration of xantphos (solid diamonds).

Moreover, a systematic study of reactions of [NiCp₂] with xantphos, **1a** and **2** in varying stoichiometric ratios indicated the formation of **7a**. The reaction of [NiCp₂] with 3 equiv of xantphos, 2 equiv of **1a** and 1 equiv of **2** produced **3a** (75 %) and **4** (<4 %), along with a small amount of **7a**. After 48 h, about 14 % of [NiCp₂] was converted into **7a** (Figure 6), which was identified by a singlet at $\delta(^1\text{H}) = 1.35$ ppm and a doublet of doublets centered at $\delta(^{31}\text{P}) = 22.0$ ppm (Figure S15).

These results suggest that the alkyne complex may be formed in the [NiCp₂]/xantphos system under N₂ and may act as the catalytically active species. It may be possible that **7a** is also relevant to the reaction in air, if it reacts more quickly with **2** than with O₂. But the catalytic reaction in air requires further study.

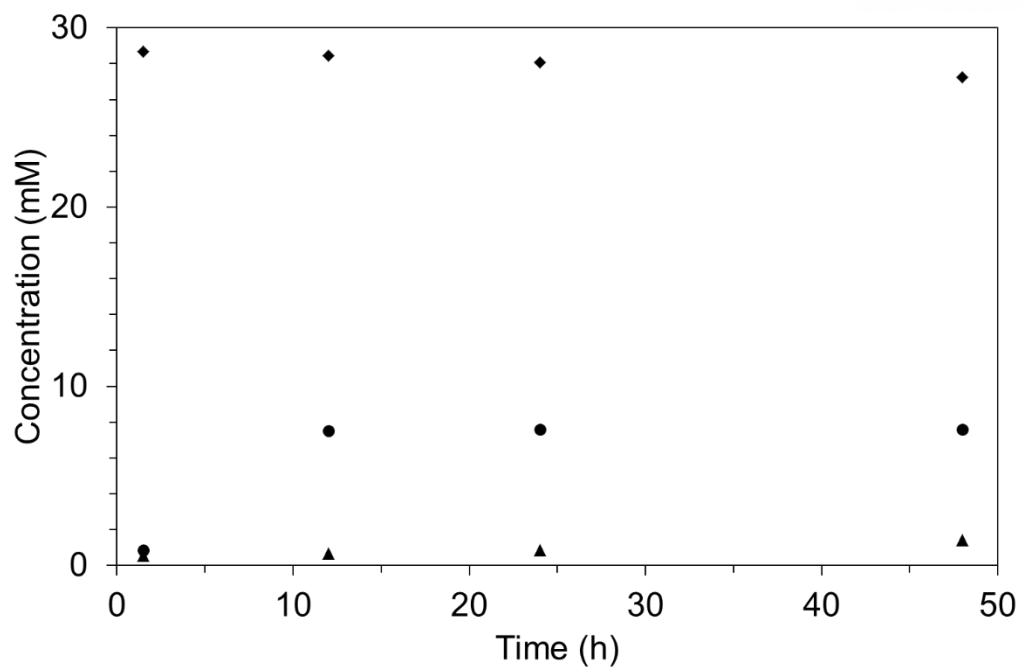


Figure 6. Time course (^1H NMR, 400 MHz, 25 $^\circ\text{C}$) of the reaction of 10 mM NiCp_2 with 3 equiv of xantphos, 2 equiv of **1a** and 1 equiv of **2** in benzene- d_6 , showing the formation of **3a** (solid circles) and **7a** (solid triangles) and the change in the concentration of xantphos (solid diamonds).

4.4 Conclusion

The Ni⁰ complexes **6**, **7a** and **7b** were found to exhibit excellent activity in the AAC under inert conditions. In reactions of **2** with the terminal alkyne **1a**, complexes **6** and **7a** produced isolated yields of over 85 % of **3a** and ≤6 % of **4**, similar to yields obtained with the [NiCp₂]/xantphos system. In reactions of **2** with the internal alkyne **1b**, complexes **6** and **7b** gave yields of over 90 % of **3b**. Interestingly, also the combination of [Ni(cod)₂] and xantphos was highly active in reactions of **2** with both **1a** and **1b**. In contrast, [Ni(cod)₂] without xantphos showed only poor activity, while the Ni^{II} complex **8** was inactive. The catalytic activity of **6** was preserved in air with either toluene or H₂O as the solvent in the presence of the additive Cs₂CO₃, which is also required in case of the [NiCp₂]/xantphos system.

Furthermore, the catalytic reactions of **6** and **7a** were investigated by NMR spectroscopy. Both complexes exhibit high catalytic activity even with a lower catalyst loading of only 1 mol %. These studies showed that **7a** is present during the catalytic reaction in both cases. Reactions of these complexes with individual substrates revealed that **6** reacts with **1a** to afford **7a** under release of one of the two xantphos ligands and that the alkyne complex rapidly reacts with benzylazide to form **3a** and **4**. Moreover, **6** also reacts with **2** under release of xantphos, but this reaction is slower than that with **1a**. A systematic study of reactions of [NiCp₂] with xantphos, **1a** and **2** in varying stoichiometric ratios indicated the formation of **6** and **7a**. These results suggest that the alkyne complex may be formed in the [NiCp₂]/xantphos system and may act as the catalytically active species.

While the NMR studies presented herein were focused on the AAC with the terminal alkyne **1a**, an investigation of the AAC with the internal alkyne **1b** is also warranted. This work is ongoing. Another direction of future study is the elucidation of the mechanism of the transformation of [NiCp₂] into **6** and **7a**.

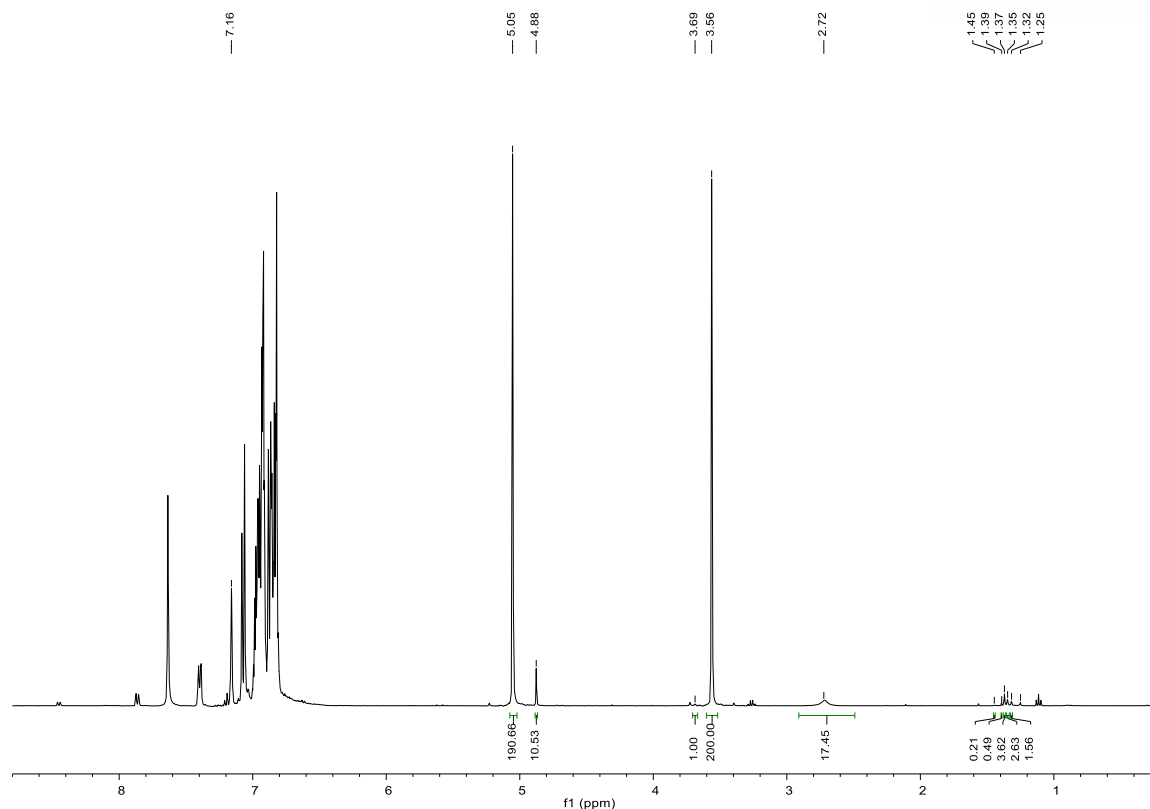


Figure S8. ¹H NMR spectrum of the product solution ($t = 51$ min) of the reaction of 100 mM **2** with 1.2 equiv of **1a** in the presence of 1 mM (1 mol %) **6** in benzene-*d*₆ (400 MHz, 25 °C).

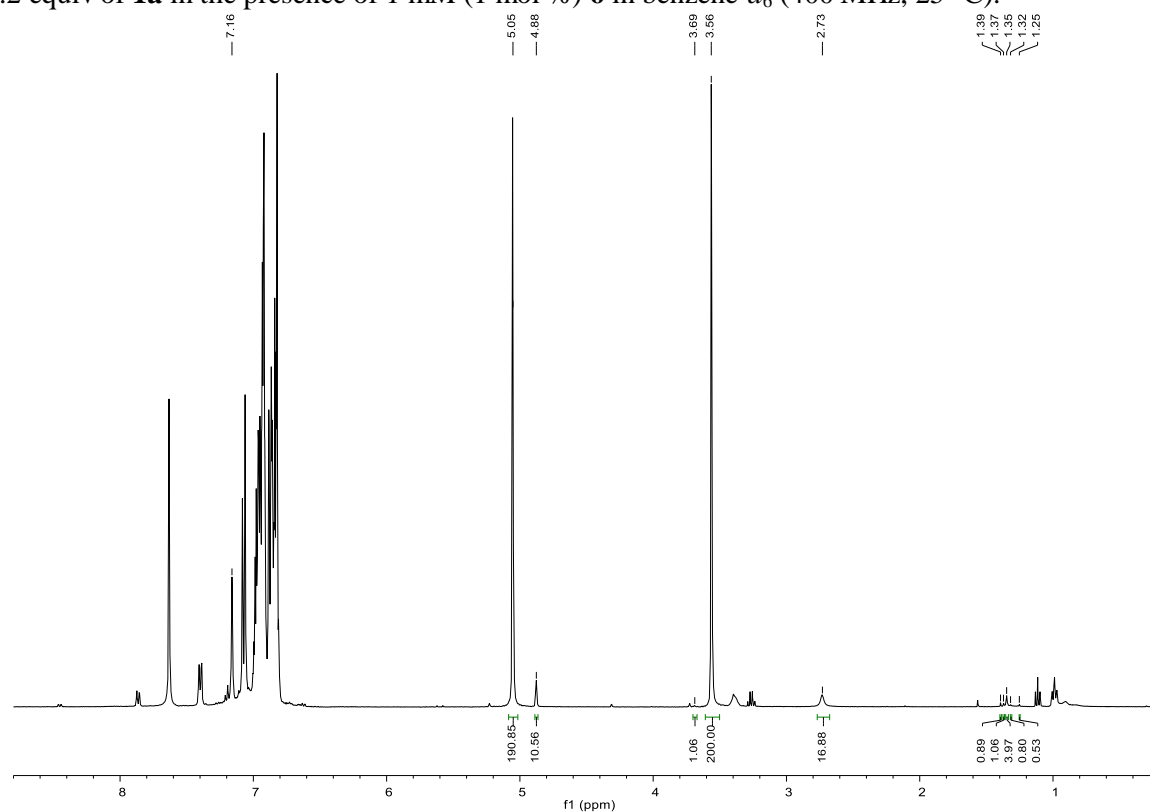


Figure S9. ¹H NMR spectrum of the product solution ($t = 19$ min) of the reaction of 100 mM **2** with 1.2 equiv of **1a** in the presence of 1 mM (1 mol %) **7a** in benzene-*d*₆ (400 MHz, 25 °C).

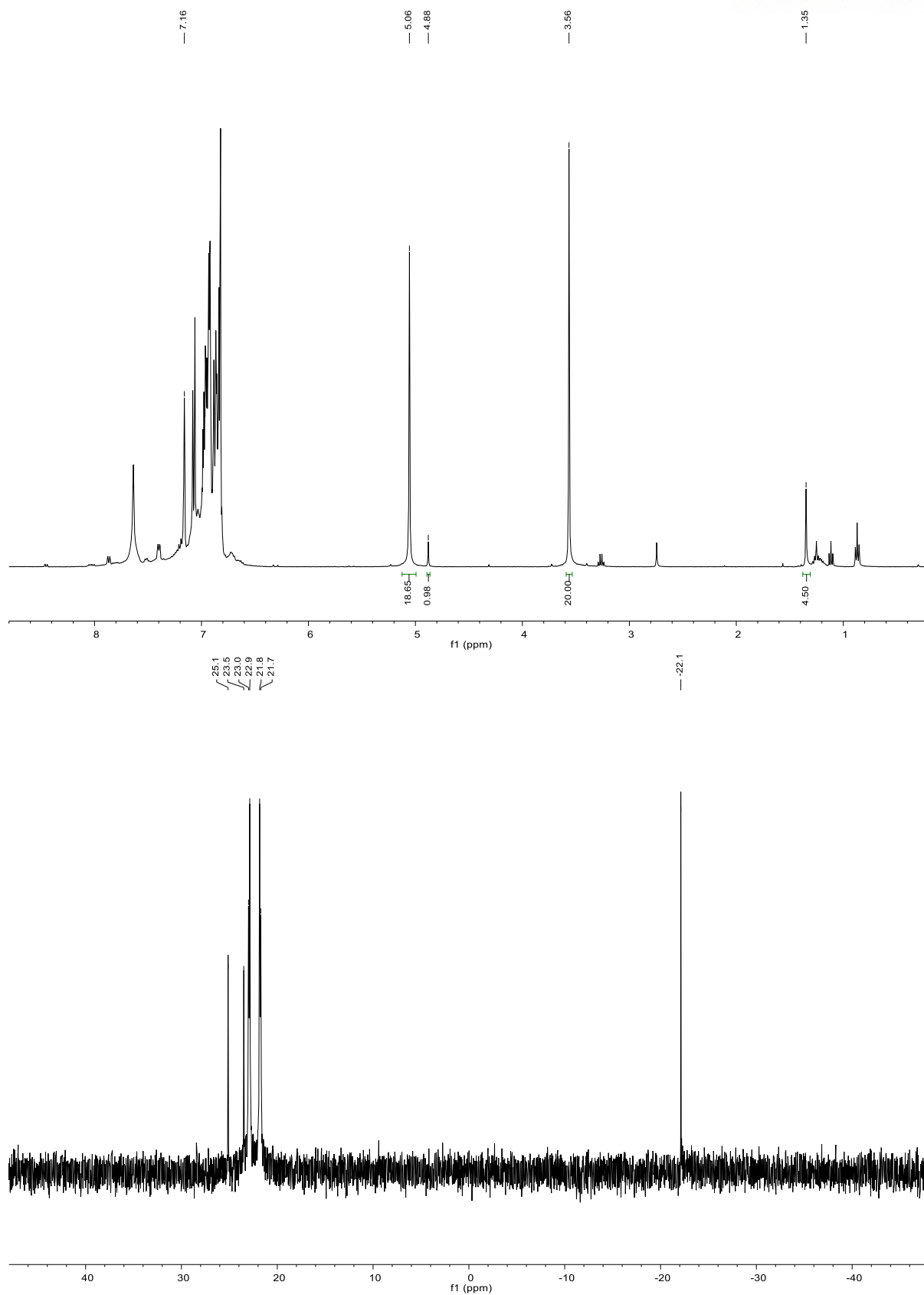


Figure S10. NMR spectra of the product solution ($t = 15$ min) of the reaction of 100 mM **2** with 1.2 equiv of **1a** in the presence of 10 mM (10 mol %) **7a** in benzene- d_6 . Top: ^1H NMR spectrum (400 MHz, 25 °C). Bottom: ^{31}P NMR spectrum (162 MHz, 25 °C).

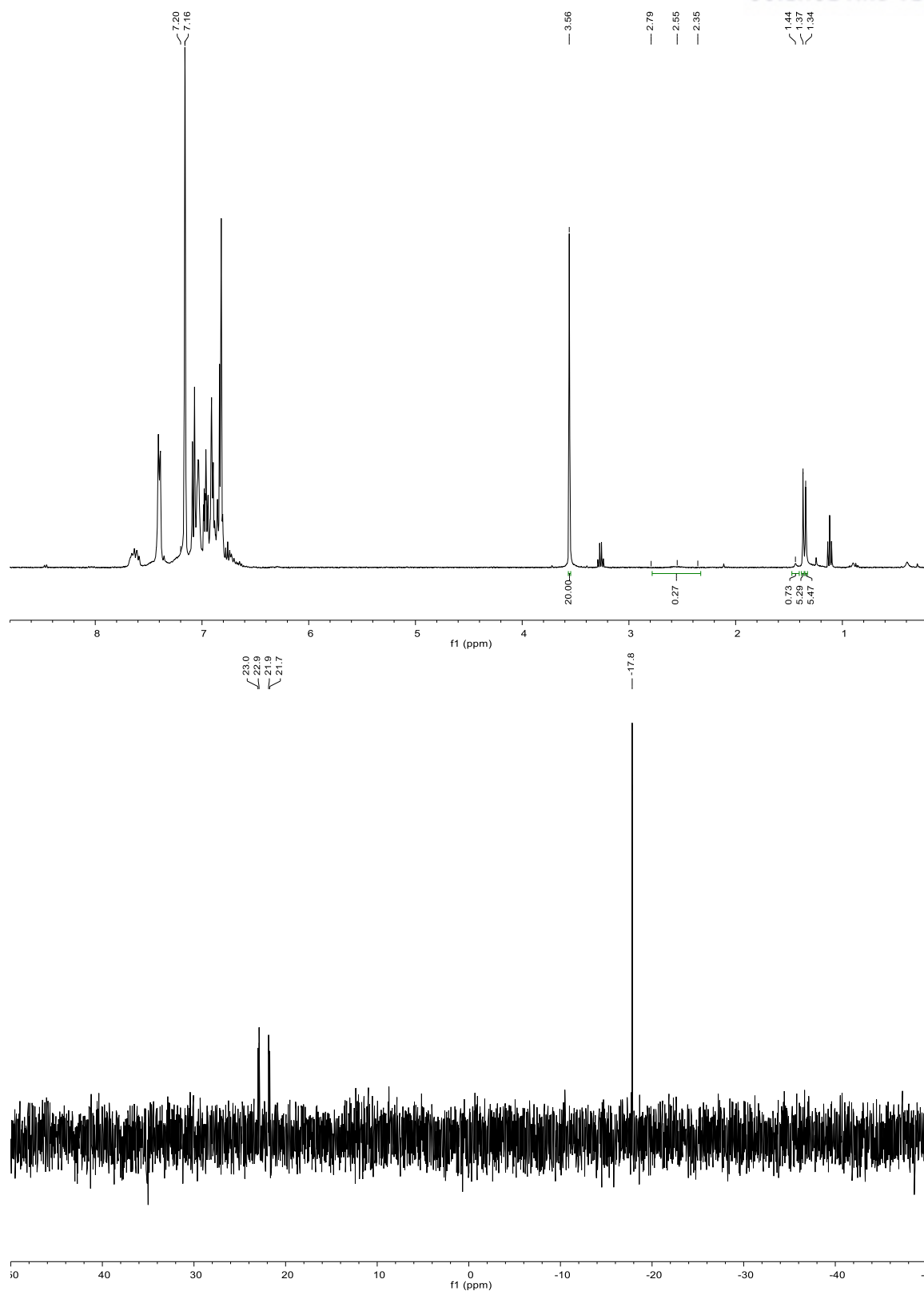


Figure S11. NMR spectra of the product solution ($t = 115$ min) of the reaction of 1 mM **6** with 10 equiv of **1a** in benzene- d_6 . Top: ^1H NMR spectrum (400 MHz, 25 °C). Bottom: ^{31}P NMR spectrum (162 MHz, 25 °C).

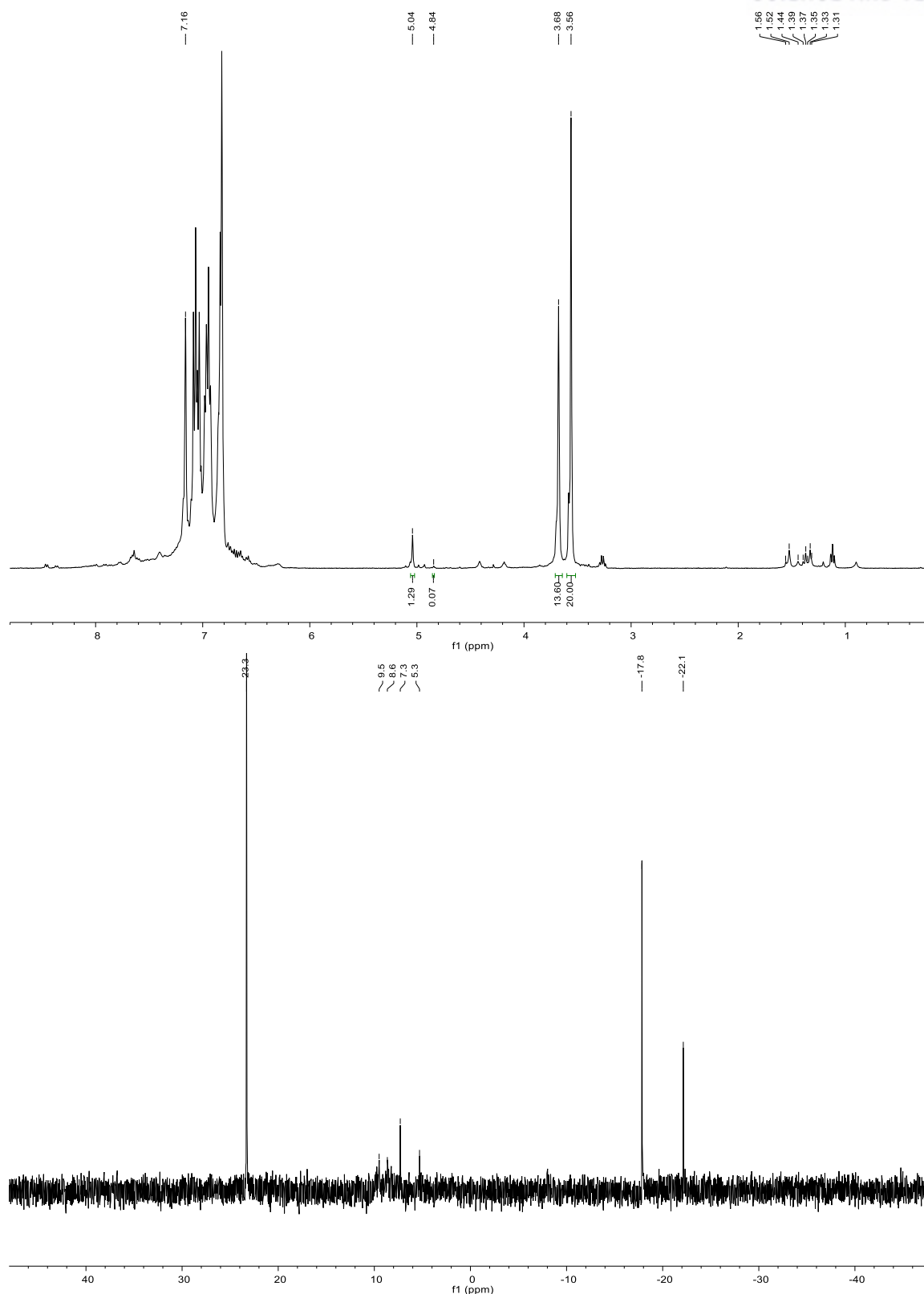


Figure S12. NMR spectra of the product solution ($t = 4$ min) of the reaction of 10 mM **7a** with 10 equiv of **2** in benzene- d_6 . Top: ^1H NMR spectrum (400 MHz, 25 °C). Bottom: ^{31}P NMR spectrum (162 MHz, 25 °C).

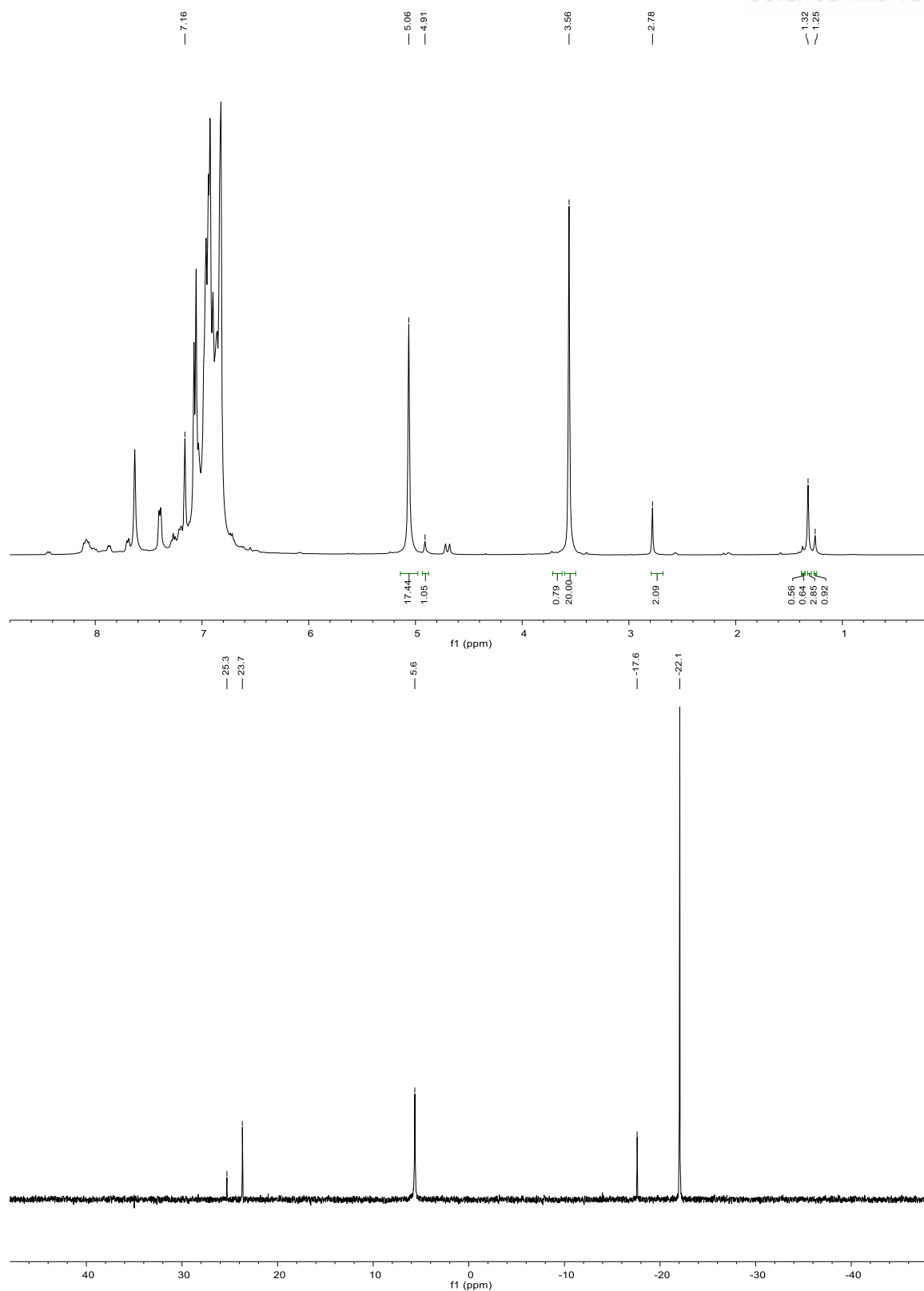


Figure S13. NMR spectra of the product solution ($t = 6$ h) of the reaction of 200 mM **2** with 1.2 equiv of **1a** in the presence of 20 mM (10 mol %) NiCp_2 and xantphos in benzene- d_6 . Top: ^1H NMR spectrum (400 MHz, 25 °C). Bottom: ^{31}P NMR spectrum (162 MHz, 25 °C).

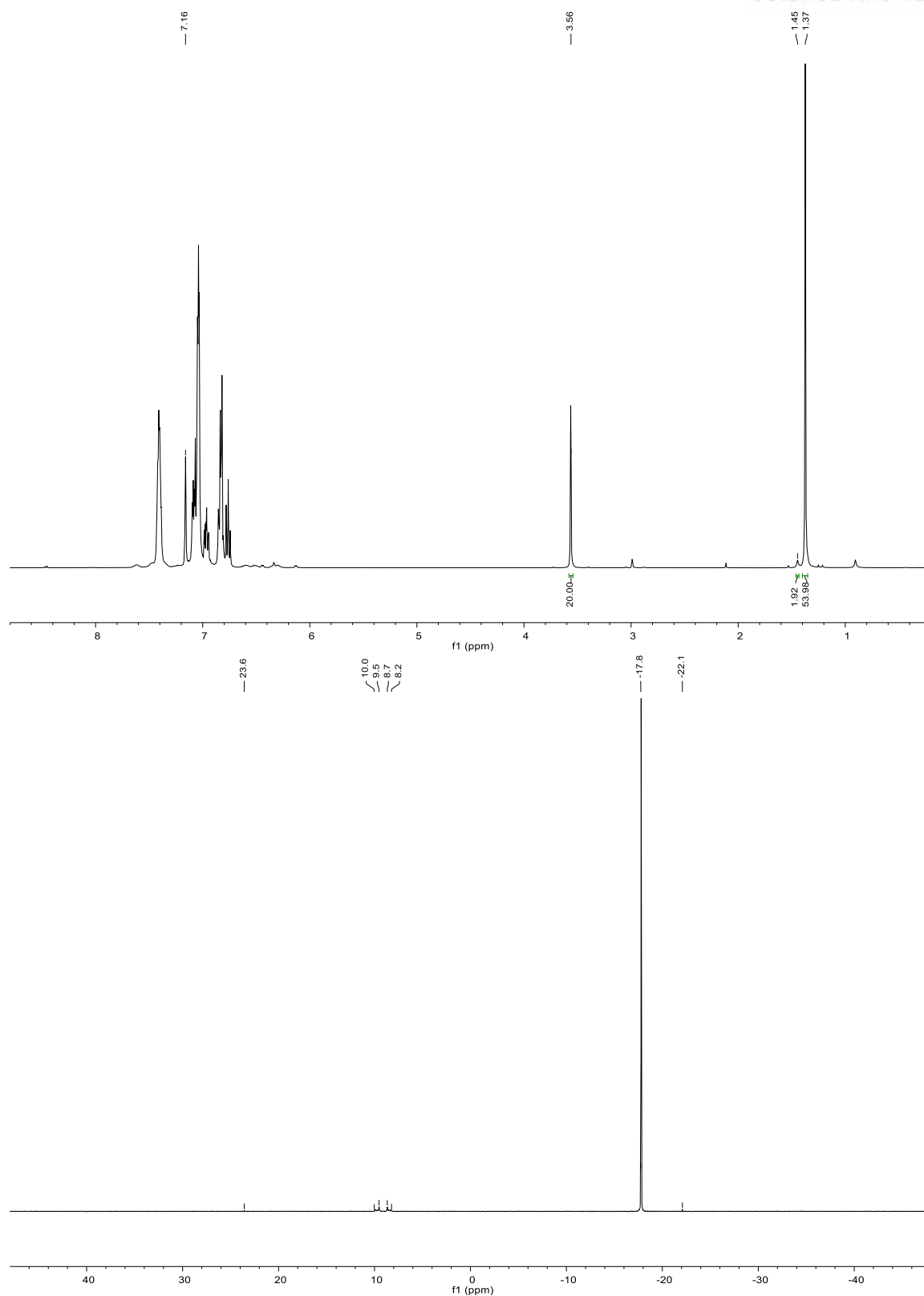


Figure S14. NMR spectra of the product solution ($t = 48$ h) of the reaction of 10 mM NiCp_2 with 10 equiv of xantphos in benzene- d_6 . Top: ^1H NMR spectrum (400 MHz, 25 °C). Bottom: ^{31}P NMR spectrum (162 MHz, 25 °C).

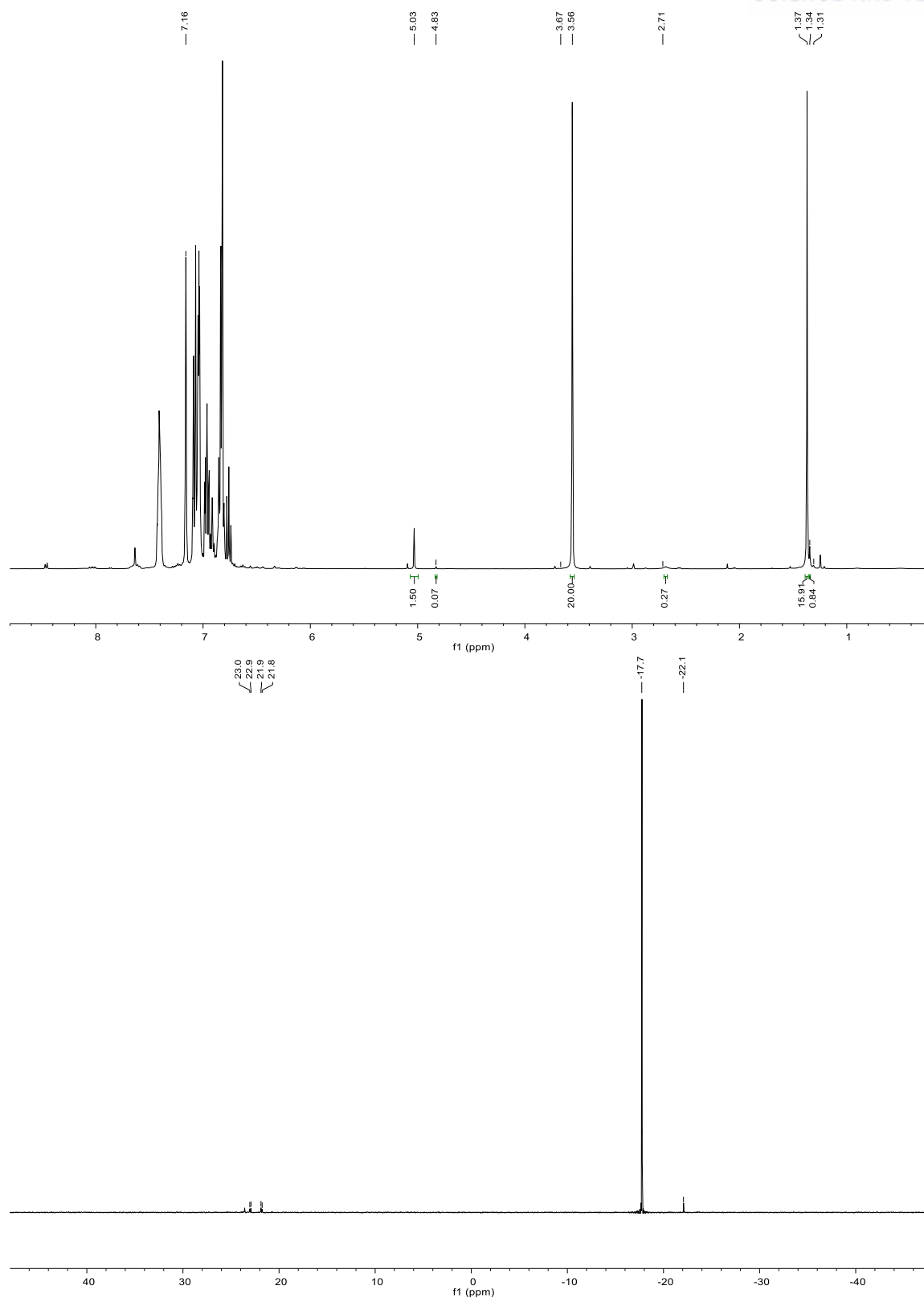


Figure S15. NMR spectra of the product solution ($t = 48$ h) of the reaction of 10 mM NiCp_2 with 3 equiv of xantphos, 2 equiv of **1a** and 1 equiv of **2** in benzene- d_6 . Top: ^1H NMR spectrum (400 MHz, 25 °C). Bottom: ^{31}P NMR spectrum (162 MHz, 25 °C).

Chapter 5

Summary and Conclusion

The synthesis and reactivity of xantphos complexes of Ni for the NiAAC was studied. The bis(chelate) complex **6** was synthesized by a substitution reaction of the Ni⁰ precursor [Ni(cod)₂] with the phosphine ligand, and its ³¹P NMR spectrum agrees with that previously reported for this complex generated *in situ*.^{16b} The new alkyne complex **7a** was synthesized by two methods, one involving substitution of the terminal alkyne **1a** for the internal alkyne ligand in **7b** and another involving substitution of **1a** for one of the xantphos ligands in **6**. The complex was characterized by ¹H and ³¹P NMR spectroscopy, elemental analysis and mass spectrometry. While the synthesis and characterization of the alkyne complex **7b** was reported previously,^{16a} an alternative method was utilized here. This method involves the sequential addition of an excess of **1b** and a stoichiometric amount of xantphos to [Ni(cod)₂]. This method is operationally simpler than the literature method, because it does not require the addition of benzonitrile to catalyze the substitution reaction. The synthesis of the Ni^{II} complex **8** was based on a method¹⁹ for its preparation as an intermediate that was used without purification and characterization. This method involves the complexation of NiCl₂·6H₂O with xantphos. Here, **8** was isolated after recrystallization, and its composition was confirmed by elemental analysis and mass spectrometry.

The catalytic activity of these complexes was explored in reactions of **2** with the terminal alkyne **1a** and the internal alkyne **1b** in toluene under inert conditions. In case of the terminal alkyne, the Ni⁰ complexes **6** and **7a** produced isolated yields of over 85 % of **3a** and ≤6 % of **4**, similar to yields obtained with the [NiCp₂]/xantphos system. When the internal alkyne was used, yields of over 85 % of **3b** were obtained. In contrast, [Ni(cod)₂] and **8** gave at best poor yields (<20 %) but in most cases only trace amounts of the 1,2,3-triazoles. The catalytic activity of **6** was preserved in air with either toluene or H₂O as the solvent in the presence of the additive Cs₂CO₃, which is also required in case of the [NiCp₂]/xantphos system.

Furthermore, the catalytic reactions of **6** and **7a** were investigated by NMR spectroscopy. Both complexes exhibit high catalytic activity even with a lower catalyst loading of only 1 mol %. These studies showed that **7a** is present during the catalytic reaction in both cases. Based on these catalytic and additional stoichiometric studies, a tentative mechanism for the AAC catalysis by these complexes was proposed. A systematic study of reactions of [NiCp₂] with xantphos, **1a** and **2** in varying stoichiometric ratios indicated the formation of **6** and **7a**. These results suggest that the alkyne complex may be formed in the [NiCp₂]/xantphos system and may act as the catalytically active

species.

While the NMR studies presented herein were focused on the AAC with the terminal alkyne **1a**, an investigation of the AAC with the internal alkyne **1b** is also warranted. This work is ongoing. Another direction of future study is the elucidation of the mechanism of the conversion of [NiCp₂] into **6** and **7a**.

References

1. A. Michael, *J. Prakt. Chem.* **1893**, 48, 94-95.
2. R. Huisgen, *Angew Chem. Int. Ed.* **1963**, 75, 604-637.
3. R. Huisgen, *Angew Chem. Int. Ed.* **1963**, 75, 742-745
4. F. Himo, T. Lovell, R. Hilgraf, V. V. Rostovtsev, L. Noodleman, K. B. Sharpless, V. V. Fokin, *J. Am. Chem. Soc.* **2005**, 127, 210-216.
5. C. W. Tornøe, M. Meldal in *Peptides 2001*, Proc. Am. Pept. Symp., American Peptide Society and Kluwer Academic Publishers, San Diego, 2001, pp. 263–264.
6. C. W. Tornoe, C. Christensen, M. Meldal, *J. Org. chem.* **2002**, 67, 3057-3064.
7. V. V. Rostovtsev, L. G. Green, V. V. Fokin, K. B. Sharpless, *Angew. Chem. Int. Ed.* **2002**, 41, 2596-2599.
8. C. Shao, G. Cheng, D. Su, J. Xu, X. Wang, Y. Hu, *Synth. Catal.* **2010**, 352, 1587–1592
9. W. S. Brotherton, H. A. Michaels, J. T. Simmons, R. J. Clark, N. S. Dalal, L. Zhu, *Org. let.* **2009**, 11, 4954-4957.
10. L. Zhu, C. J. Brassard, X. Zhang, P. M. Guha, R. J. Clark, *Chem. Rec.* **2016**, 16, 1501-1517.
11. L. Zhang, X. Chen, P. Xue, H. H. Sun, I. D. Williams, K. B. Sharpless, V. V. Fokin, G. Jia, *J. Am. Chem. Soc.* **2005**, 127, 15998-15999.
12. B. C. Boren, S. Narayan, L. K. Rasmussen, L. Zhang, H. Zhao, Z. Lin, G. Jia, V. V. Fokin, *J. Am. Chem. Soc.* **2008**, 130, 8923-8930.
13. W. G. Kim, M. E. Kang, J. B. Lee, M. H. Jeon, S. Lee, J. Lee, B. Choi, P. Cal, S. Kang, J. M. Kee, G. J. L. Bernardes, J. U. Rohde, W. Choe, S. Y. Hong, *J. Am. Chem. Soc.* **2017**, 139, 12121-12124.

14. W. L. F. Armarego, C. L. L. Chai, *Purification of Laboratory Chemicals*, 6th ed.; Butterworth-Heinemann: Oxford, U.K., **2009**.
15. J. Lee, J.-U. Rohde, Ulsan National Institute of Science and Technology, Ulsan, Republic of Korea. Unpublished work, 2018.
16. (a) N. D. Staudaher, R. M. Stolley, J. Louie, *Chem. Commun.* **2014**, 50, 15577-15580. (b) R. M. Stolley, Ph. D. Dissertation, The University of Utah, U.S.A., **2014**.
17. T. Saito, H. Munakata H. Imoto, A. Davison, K. Jonas, B. Albiez, *Inorg. Synth.* **1977**, 17, 83-88
18. A. F. Orsino, M. Gutierrez Del Campo, M. Lutz, M. E. Moret, *ACS Catal.* **2019**, 9, 2458-2481.
19. E. A. Standley, S. J. Smith, P. Muller, T. F. Jamison, *Organometallics* **2014**, 33, 2012-2018.
20. W. D. G. Brittain, B. R. Buckley, J. S. Fossey, *Chem. Commun.* **2015**, 51, 17217-17220.
21. E. Kent Barefield, D A. Krost, D. S. Edwards, D. G. Van Derveer, R. L. Trytko, S. P. O'Rear, Alex N. Williamson *J. Am. Chem. Soc.* **1981**, 103, 20, 6219-6222.
22. E. Uhlig, H. Walther, *Z. Anorg. Allg. Chem.* **1974**, 409, 89.
23. J. R. Olechowski, C. G. McAlister, R. F. Clark, *Inorg. Chem.* **1965**, 4, 246.
24. N. E. Leadbeater, *J. Org. Chem.* **2001**, 66, 7539-7541.